

AD _____

Award Number: DAMD17-01-1-0776

TITLE: Biochemical Markers for Exposure to Low Doses of
Organophosphorus Insecticides

PRINCIPAL INVESTIGATOR: Oksana Lockridge, Ph.D.

CONTRACTING ORGANIZATION: University of Nebraska Medical Center
Omaha, Nebraska 68198-6810

REPORT DATE: August 2002

TYPE OF REPORT: Annual

PREPARED FOR: U.S. Army Medical Research and Materiel Command
Fort Detrick, Maryland 21702-5012

DISTRIBUTION STATEMENT: Approved for Public Release;
Distribution Unlimited

The views, opinions and/or findings contained in this report are those of the author(s) and should not be construed as an official Department of the Army position, policy or decision unless so designated by other documentation.

20021127 105

REPORT DOCUMENTATION PAGEForm Approved
OMB No. 074-0188

Public reporting burden for this collection of information is estimated to average 1 hour per response, including the time for reviewing instructions, searching existing data sources, gathering and maintaining the data needed, and completing and reviewing this collection of information. Send comments regarding this burden estimate or any other aspect of this collection of information, including suggestions for reducing this burden to Washington Headquarters Services, Directorate for Information Operations and Reports, 1215 Jefferson Davis Highway, Suite 1204, Arlington, VA 22202-4302, and to the Office of Management and Budget, Paperwork Reduction Project (0704-0188), Washington, DC 20503

1. AGENCY USE ONLY (Leave blank)**2. REPORT DATE**

August 2002

3. REPORT TYPE AND DATES COVERED

Annual (1 Aug 01 - 31 Jul 02)

4. TITLE AND SUBTITLE

Biochemical Markers for Exposure to Low Doses of Organophosphorus Insecticides

5. FUNDING NUMBERS

DAMD17-01-1-0776

6. AUTHOR(S)

Oksana Lockridge, Ph.D.

7. PERFORMING ORGANIZATION NAME(S) AND ADDRESS(ES)University of Nebraska Medical Center
Omaha, Nebraska 68198-6810

E-Mail: olockrid@unmc.edu

**8. PERFORMING ORGANIZATION
REPORT NUMBER****9. SPONSORING / MONITORING AGENCY NAME(S) AND ADDRESS(ES)**U.S. Army Medical Research and Materiel Command
Fort Detrick, Maryland 21702-5012**10. SPONSORING / MONITORING
AGENCY REPORT NUMBER****11. SUPPLEMENTARY NOTES****12a. DISTRIBUTION / AVAILABILITY STATEMENT**

Approved for Public Release; Distribution Unlimited

12b. DISTRIBUTION CODE**13. Abstract (Maximum 200 Words) (abstract should contain no proprietary or confidential information)**

Though acetylcholinesterase is the primary target of organophosphorus toxicants, our finding that acetylcholinesterase knockout mice are supersensitive to the lethal effects of VX, DFP, chlorpyrifos oxon, and iso-OMPA demonstrates that other important targets exist. The goal of this work is to identify non-acetylcholinesterase targets of organophosphorus toxicants. Biotinylated-organophosphate was used to label proteins in mouse brain. The labeled proteins were separated by polyacrylamide gel electrophoresis and visualized with avidin conjugated to a fluorophore. This method has yielded 29 organophosphorus-reactive protein bands in mouse brain. They range in size from 15 to 100 kDa. Rate constants for reaction with biotinylated organophosphate were measured for the 29 proteins as well as for purified human acetylcholinesterase and human butyrylcholinesterase. A method has been developed to screen proteins for reactivity with organophosphorus agents. This work is expected to identify new biological markers for low dose exposure to organophosphorus toxicants and to explain the neurologic symptoms of some of our Gulf War veterans.

14. SUBJECT TERMS

Gulf War Illness, insecticide, nerve agent, acetylcholinesterase, low dose, biochemical markers, organophosphorus toxicant

15. NUMBER OF PAGES

59

16. PRICE CODE**17. SECURITY CLASSIFICATION
OF REPORT**

Unclassified

**18. SECURITY CLASSIFICATION
OF THIS PAGE**

Unclassified

**19. SECURITY CLASSIFICATION
OF ABSTRACT**

Unclassified

20. LIMITATION OF ABSTRACT

Unlimited

NSN 7540-01-280-5500

Standard Form 298 (Rev. 2-89)
Prescribed by ANSI Std. Z39-18
298-102

Table of Contents

Cover.....	1
SF 298.....	2
Table Of Contents	3
Abbreviations	4
Introduction	5
Body.....	5-43
Task 1.....	5-11
Task 2.....	12-21
Task 3.....	22-32
Task 5.....	33-43
Key Research Accomplishments.....	44
Reportable Outcomes	44
Conclusions.....	44
References.....	45-46
Appendices	46-59

Abbreviations

AChE	acetylcholinesterase enzyme
BChE	butyrylcholinesterase enzyme
BSA	bovine serum albumin
CHO	Chinese Hamster Ovary Cells
CPO	chlorpyrifos oxon
DFP	diisopropylfluorophosphate
DTNB	dithiobisnitrobenzoic acid
FP-biotin	biotinylated organophosphate where the leaving group is the fluoride ion and the marker is biotin; 10-(fluoroethoxyphosphoryl)-N-(biotinamidopentyl) decanamide
IC50	the concentration of inhibitor necessary to obtain 50% inhibition
iso-OMPA	tetraisopropyl pyrophosphoramidate
OP	organophosphorus toxicant
QNB	3H-quinuclidinyl benzilate, ligand for muscarinic receptors
SDS	sodium dodecyl sulfate
VX	O-ethyl S-[2-(diisopropylamino)ethyl] methylphosphonothioate; nerve agent

Introduction. The purpose of this work is to identify proteins that react with low doses of organophosphorus agents (OP). There is overwhelming evidence that acute toxicity of OP is due to inhibition of AChE. However, we have found that the AChE knockout mouse, which has zero AChE, is supersensitive to low doses of OP. The AChE $-/-$ mouse dies at doses of OP that are not lethal to wild-type mice (Duysen et al., 2001; Duysen et al., 2002). This demonstrates that non-AChE targets are involved in OP toxicity. Our goal is to identify new biological markers of exposure to organophosphorus agents.

Our strategy uses biotinylated OP to label proteins, which are then visualized with avidin conjugated to a fluorophore. Proteins that react faster than AChE with OP will be identified by mass spectrometry and amino acid sequencing.

Since some cases of Gulf War Illness may have been caused by exposure to low doses of OP, our studies may lead to an explanation for the neurologic symptoms in some of our Gulf War veterans.

Relation to Statement of Work. This year, the first year of the project, we have made progress on Tasks 1, 2, 3, and 5.

Task 1.

Biotinylated OP will be synthesized in the laboratory of Dr. Charles Thompson at the University of Montana. 1-20 mg of biotinylated OP will be provided to Dr. Lockridge.

Task 1 has been completed.

Abstract. A biotinylated OP was synthesized in the laboratory of Dr. Charles Thompson at the University of Montana. The FP-biotin was found to be

stable in methanol but unstable in water. The rate constant for reaction with human AChE was $3.0 \times 10^6 \text{ M}^{-1}\text{min}^{-1}$, and for human BChE was $2 \times 10^8 \text{ M}^{-1}\text{min}^{-1}$. A minor stereoisomer, constituting about 10% of the FP-biotin preparation, appeared to be reacting with BChE.

Introduction. We decided to use biotinylated OP to fish out proteins that react with OP because the biotin label not only marks the protein but also allows one-step purification of biotinylated proteins on avidin conjugated to Sepharose. After we made this decision we found that Liu et al (1999) had published a method for synthesizing the compound we wanted. Therefore, we adapted their synthesis scheme to make FP-biotin. We are using the FP-biotin to test our hypothesis. Our hypothesis is that proteins other than AChE react with low doses of insecticide OP, and that these reactions cause toxicity.

Methods and Results

Synthesis of FP-biotin. Troy Voelker, in Dr. Thompson's laboratory, synthesized, purified, and sent to us 15.5 mg of 10-(fluoroethoxyphosphophenyl)-N-(biotinamidopentyl) decanamide (FP-biotin). See Figure 1.1.

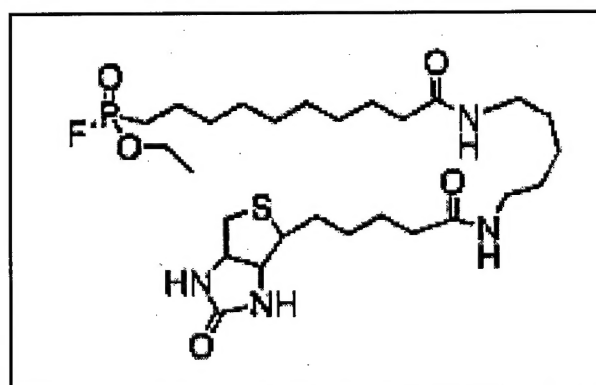


Figure 1.1. FP-biotin structure. The OP has a reactive phosphonofluoridate group tethered to biotin via a spacer arm.

The steps in the synthesis of FP-biotin are shown in Figure 1.2. They follow the procedure of Liu et al. (1999). 1-Hydroxy-10-undecene (**2**) was reacted with toluenesulfonyl chloride in pyridine to form the corresponding tosylate (**3**). Displacement of the tosylate with iodide formed 1-iodo-10-undecene (**4**), which was reacted with triethylphosphite to form 1-(diethoxyphosphonyl)-10-undecene (**5**). Monodealkylation of one of the ethyl esters with TMS-Br formed the

phosphorus monoacid (**6**). Ruthenium chloride-promoted oxidative cleavage resulted in formation of the decanoic acid (**7**). The acid **7** was converted to the phosphonofluoridate **8** using DAST and then coupled to 5-(biotinamido)-pentylamine (BAPA; **9**; Lee, 1988) to form FP-biotin. Yield for each step was noted except for the final two transformations, which are combined (Liu et al., 1999). The overall yield for the multistep synthesis was estimated to be about 6%.

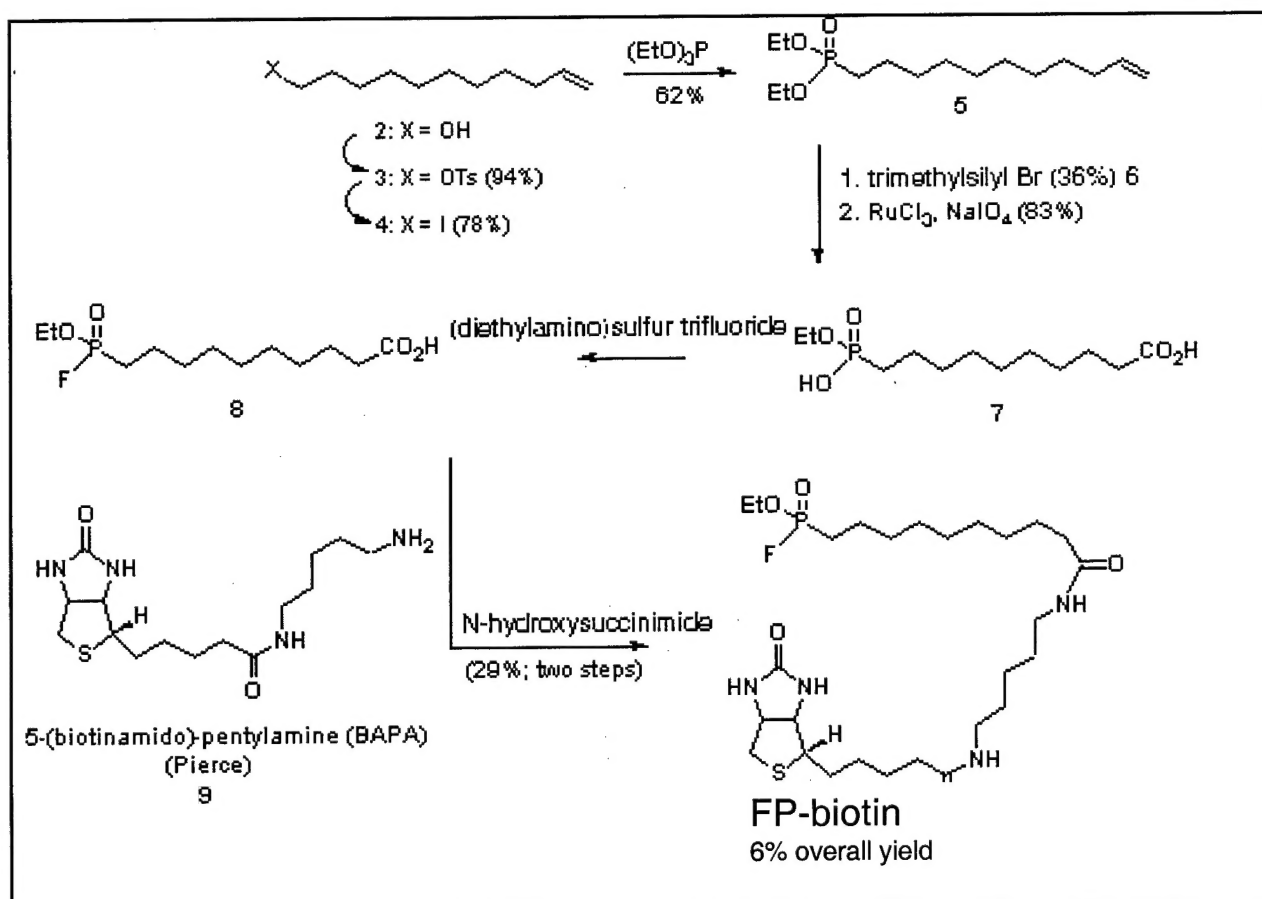


Figure 1.2. Synthesis of FP-biotin.

Purification and characterization of FP-biotin. FP-biotin was purified by washing the crystals sequentially with diethyl ether and ethyl acetate.

The identity of the biotinylated OP and of the intermediates was confirmed by ^1H -NMR, ^{13}C -NMR and ^{31}P -NMR, absorbance spectra in the UV-Vis wavelength range, and combustion analysis. Phosphorous NMR showed a doublet (36.0 and 29.3 ppm from H_3PO_4)

as expected. Mass spectrometry (TOF MS ES+) showed that FP-biotin had a mass to charge ratio of 593.5 (m/z). The expected m/z for FP-biotin, $C_{27}FH_{50}N_4O_5PS + H^+$, is 593.3. There was a peak at 297.3 (m/z), i.e. 1/2 of the major peak, and at 615.6 (m/z), i.e. the major peak plus one sodium. No evidence for contamination was detected.

Storage of FP-biotin. The FP-biotin arrived dry, in two sealed glass ampoules (7.1 mg and 8.4 mg), and was stored at -70°C . The 7.1 mg portion was dissolved in 0.7 ml of methanol (HPLC grade, from EM Science), divided into 7 aliquots (100 μl each), which were placed into Pyrex tubes cleaned in a muffle oven. The aliquots were dried under vacuum in a Speedvac, at room temperature. Six of the seven dried aliquots were returned to storage at -70°C . One ml of methanol was added to one aliquot to give a 1 mg/ml, or 1.7 mM, stock solution of FP-biotin. This methanol stock solution was stored at -70°C .

Concentration of FP-biotin. The concentration of biotin in the FP-biotin stock solution was checked by titration against a complex of avidin (Sigma) and HABA (4-hydroxy azobenzene-2-carboxylic acid, from Sigma) as described by Green (1965). The titration yielded a concentration for biotin in the methanol stock solution of 1.78 mM or 105% of the expected concentration obtained by weight.

Stability of FP-biotin. The stability of FP-biotin in water was assessed by its ability to inhibit BChE activity. Stock FP-biotin (1.7 mM in methanol) was diluted 1000-fold into water to yield a 1.7 μM test solution of FP-biotin at zero time. Test solutions were stored at room temperature in capped vials (either Pyrex or white plastic microfuge tubes from Midwest Scientific). The

apparent first-order rate constant for FP-biotin inhibition of BChE was determined by incubating 20 μl aliquots of the FP-biotin test solution with 1.87 ml of BChE (in 0.1 M potassium phosphate buffer pH 7.0, at 25°C) for defined times, ranging from 0 to 20 minutes (Figure 1.3 inset).

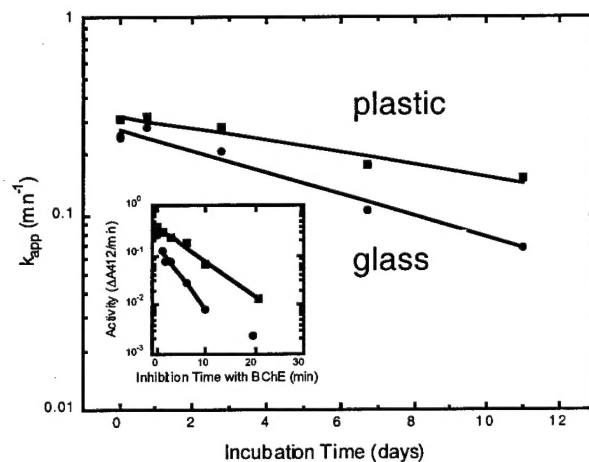


Figure 1.3. Decay of FP-biotin in water. Incubation time is the time for which FP-biotin was left at room temperature; k_{app} is the apparent first-order rate constant for the inhibition of BChE by FP-biotin. Squares show the results for FP-biotin stored in a plastic microfuge tube, circles for storage in a Pyrex tube. Lines are from fits to a first-order process.

Inset: The inhibition of BChE by FP-biotin on day-0 (circles) and day-11 (squares), from incubation in plastic. Lines are from fits to a first-order process. Data were fit using SigmaPlot (Jandel).

Active BChE remaining at the end of each incubation was determined according to the method of Ellman et al., [1961], i.e. turnover was initiated by addition of butyrylthiocholine to a final concentration of 1 mM, and dithiobis-p-nitrobenzoic acid (DTNB) to 0.5 mM. Product formation was recorded in a spectrophotometer at 412

nm. Semi-log plots of {inhibition time} versus {residual activity} were linear for at least 90% of the reaction, from which apparent first-order rate constants for FP-biotin inhibition could be determined (Figure 1.3 inset). The inhibition potency of the FP-biotin test solution decreased with time of storage at room temperature. A plot of the {apparent first-order rate constant for FP-biotin inhibition of BChE turnover} versus {the storage time for the FP-biotin test solution} decreased in a first-order fashion (Figure 1.3). The half-life for loss of FP-biotin was 5.5 ± 0.4 days (in glass) or 9.9 ± 1.5 days (in plastic). Aqueous stock solutions of FP-biotin are stored routinely in white plastic microfuge tubes from Midwest Scientific.

Reaction of FP-biotin with human AChE.

The kinetics for the inhibition of purified human AChE by FP-biotin were studied in 0.1 M potassium phosphate buffer pH 7.0 at 25°C. Bovine serum albumin (BSA), normally included to stabilize AChE, was omitted because it reduced the apparent first-order inhibition constant measured with FP-biotin. Inhibition of AChE was initiated by mixing 0.17 nM AChE (recombinant, from CHO-K1 cells) with variable amounts of FP-biotin. At defined times, inhibition was quenched and residual AChE activity was determined by adding 0.5 mM DTNB and 1.0 mM acetylthiocholine [Ellman et al., 1961]. Inhibition of AChE was first-order for at least 90% of the reaction (Figure 1.4, inset). A plot of {the apparent first-order rate constant for inhibition} versus {the concentration of FP-biotin} was linear from 0.025 to 0.25 μM FP-biotin (Figure 1.4). The apparent second-order rate constant for the reaction of human AChE with FP-

biotin was $3.0 \times 10^6 \pm 3.9 \times 10^4 \text{ M}^{-1} \text{ min}^{-1}$.

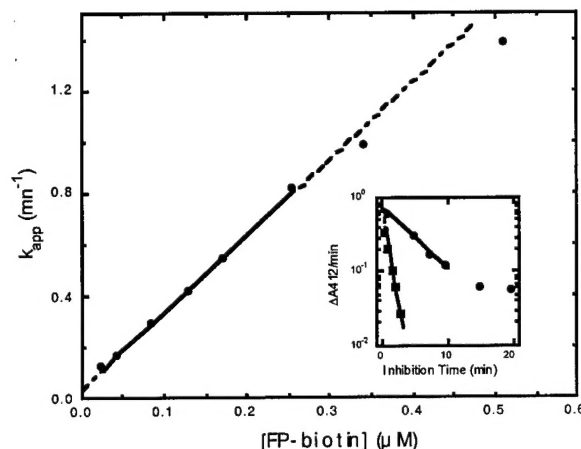


Figure 1.4. Rate constant for inhibition of human AChE by FP-biotin. k_{app} is the apparent first-order rate constant for the inhibition of AChE by FP-biotin. Points are the data; the solid line is from a linear fit, and the dashed line is an extrapolation of the fitted line.

Inset: Inhibition of AChE by 0.043 μM FP-biotin (circles) and 0.34 μM FP-biotin (squares). Solid lines are from fits to a first-order process. Data were fit using SigmaPlot.

Extrapolation of the second-order line to zero FP-biotin revealed a small non-zero Y-axis intercept, which is consistent with a minor, spontaneous loss of AChE activity due to the absence of BSA. For FP-biotin concentrations greater than 0.3 μM , the apparent first-order rate constants fell below the extrapolated second-order line, suggesting the onset of saturation, and the existence of a non-covalent complex between FP-biotin and AChE. Data were insufficient to estimate the dissociation constant for the non-covalent complex.

Reaction of FP-biotin with human BChE. Kinetics for the inhibition of human BChE by FP-biotin were studied in 0.1 M potassium phosphate buffer pH 7.0 at 25°C. Wild type human BChE (0.35 nM) was incubated with variable amounts of FP-biotin for defined times. Inhibition was

stopped and residual BChE activity was determined by addition of 0.5 mM DTNB and 1 mM butyrylthiocholine [Ellman et al., 1961]. Loss of BChE activity was first-order for at least 90% of the reaction, at all concentrations of FP-biotin except for the very lowest (4.3 nM). See Figure 1.5 inset.

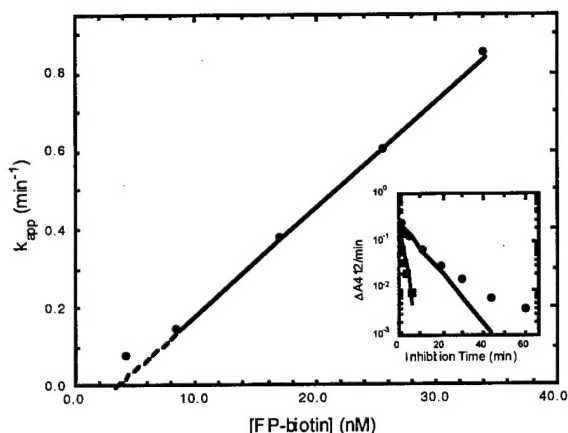


Figure 1.5. Inhibition of BChE by FP-biotin. k_{app} is the apparent first-order rate constant for the inhibition of human BChE by FP-biotin. Points are the data; the solid line is from a linear fit; the dashed line is an extrapolation of the fitted line.

Inset: The inhibition of BChE by 4.3 nM FP-biotin (circles) and 34 nM FP-biotin (squares). Solid lines are from fits to a first-order process. Data were fit using SigmaPlot.

A plot of {the apparent first-order rate constant for the loss of BChE activity} versus {FP-biotin concentration} was linear from 8.5 to 34 nM FP-biotin (Figure 1.5). The apparent second-order rate constant for the reaction of human BChE with FP-biotin was $2.8 \times 10^7 \pm 3.0 \times 10^5 \text{ M}^{-1} \text{ min}^{-1}$.

Extrapolation of the second-order line to a rate constant of zero gave a non-zero X-axis intercept of 3.5 nM. This non-zero X-axis intercept suggests that the reactions are not in the pseudo-first order range, despite the fact that the concentration of BChE in the reaction was 0.35 nM and the

minimum concentration of FP-biotin was 4.3 nM. This in turn suggests that BChE was reacting with a minor component of the FP-biotin preparation. The X-axis intercept should yield the concentration of the fixed member of the reaction (BChE in this case). In order to make this so, the concentration of the reactive species in the FP-biotin preparation must have been 10% of the total FP-biotin concentration. A sub-stoichiometric titration of BChE with FP-biotin confirmed this prediction.

The sub-stoichiometric titration of BChE was performed by incubating FP-biotin (0.34 to 4.93 nM) with 0.42 nM BChE, until inhibition had reached its maximum extent, that is for 4 hours. Preliminary experiments indicated that 4 hours in 0.1 M potassium phosphate buffer, pH 7.0 at 25°C was sufficient incubation time to allow the inhibition reaction to come to completion. Then 0.5 mM DTNB and 1 mM butyrylthiocholine were added to the incubation mixture to determine the amount of active BChE remaining. A plot of {residual activity} versus {FP-biotin concentration} was linear to 93% inhibition, indicating stoichiometric inhibition of BChE (Figure 1.6). However, 2.7 nM FP-biotin was required to fully inhibit the 0.42 nM BChE, indicating that only 15% of the FP-biotin stock solution was involved in the inhibition.

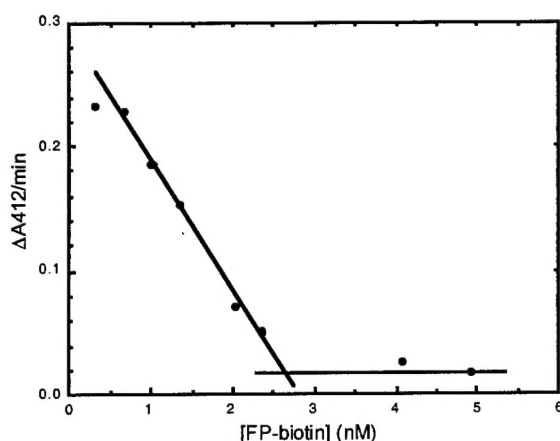


Figure 1.6. Substoichiometric titration of BChE with FP-biotin. Points are the data; lines were drawn by hand to assist in determining trends.

Though the FP-biotin appeared to be pure, a 10-15% contamination may have been undetected. To test whether intact FP-biotin was responsible for the inhibition of BChE, the inhibited BChE was checked for the presence of covalently attached biotin. It was reasoned that a contaminant in the FP-biotin preparation either would be missing the biotin moiety or would be incapable of forming a covalent adduct with BChE. 2.4 pmoles of FP-biotin-inhibited-BChE were applied to an SDS polyacrylamide gel, electrophoresed and then transferred to PVDF membrane. To measure the biotin, the membrane was treated with an avidin-horseradish peroxidase conjugate (BioRad), and then with a chemiluminescence reagent (LumiGLO from Kirkegaard & Perry). Emitted light was detected using x-ray film. The light intensity, which is directly proportional to the biotin level, was quantitated densitometrically using the Kodak EDAS 120 image analysis system and Kodak 1D software. Intensity was compared to a standard curve prepared by reacting a

standardized portion of trypsin (Sigma) with FP-biotin and running various sized aliquots of this reaction mixture on the same SDS gel as the inhibited BChE. The biotin signal for BChE was equivalent to 2.0 pmoles (Figure 1.7), indicating that about 83% of the inhibited BChE carried a biotin.

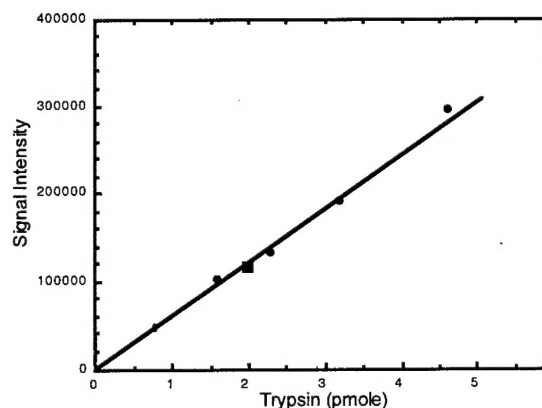


Figure 1.7. Quantitation of biotin covalently attached to BChE. The circles are the trypsin standards; the square is the BChE intensity reading. The line was drawn by hand.

Since the gel was run in SDS, the biotin must be covalently attached to the BChE. Therefore, inhibition of BChE does not appear to be due to a contaminant. An alternate explanation stems from the fact that FP-biotin is potentially a racemic mixture of phosphate stereoisomers (see the FP-biotin structure). Stereoselective inhibition by organophosphate stereoisomers has been reported for BChE [Millard et al., 1998; Doorn et al., 2001]. If BChE reacts preferentially with a minor (10%) stereoisomeric form of FP-biotin, the observed kinetics could be rationalized. In that case, the second-order rate constant for the reaction of human BChE with FP-biotin would be $2 \times 10^8 \text{ M}^{-1}\text{min}^{-1}$.

Discussion

The FP-biotin synthesized by the laboratory of Dr. Charles Thompson is a high quality reagent. It is pure by mass spectrometry and by titration with avidin. About 10% of the compound appears to be a stereoisomer of FP-biotin that preferentially reacts with human BChE. The product of the reaction with BChE is biotinylated BChE where the biotin is covalently attached to the active site of BChE through a phosphate group. This reagent is suitable for the proposed task of identifying OP reactive proteins.

FP-biotin has good reactivity with human AChE and BChE despite its large biotin group. The spacer arm and biotin group are too large to fit inside the active site gorge. We assume that the biotin either sits at the mouth of the gorge, or alternatively, that it extends through a putative backdoor.

Summary of results in Task 1.

- FP-biotin was synthesized and purified. Its structure was confirmed by mass spectrometry.
- The FP-biotin was stable in methanol but unstable in aqueous solution.
- Aqueous solutions were more stable in plastic than in glass tubes.
- The apparent second-order rate constant for the reaction of human AChE with FP-biotin was $3.0 \times 10^6 \pm 3.9 \times 10^4 \text{ M}^{-1}\text{min}^{-1}$.
- The second-order rate constant for the reaction of human BChE with FP-biotin was $2 \times 10^8 \text{ M}^{-1}\text{min}^{-1}$, a rate 100 fold-higher than that with AChE.
- The FP-biotin appeared to be a racemic mixture; BChE appeared to react preferentially with a minor (10%) stereoisomeric form of FP-biotin.

Task 2.

The toxicity of various doses of chlorpyrifos oxon, dichlorvos, diazinon-O-analog, and malathion-O-analog will be tested in mice deficient in acetylcholinesterase. The goal is to find a dose that is toxic only to AChE deficient mice (AChE +/- and AChE -/-), and is not toxic to wild-type (AChE +/+) mice.

Progress has been made on Task 2. The following is from a manuscript prepared for BioScience Review 2002 [Duysen et al, 2002a].

Abstract. The acetylcholinesterase (AChE) knockout mouse is a new tool for identifying physiologically relevant targets of organophosphorus toxicants (OP). If AChE were the only important target for OP toxicity, then mice with zero AChE would have been expected to be resistant to OP. The opposite was found. AChE -/- mice were supersensitive to DFP, chlorpyrifos oxon, iso-OMPA, and the nerve agent VX. A given OP elicited the same cholinergic signs of toxicity in mice with zero AChE as in mice with normal amounts of AChE. This implied that the mechanism of toxicity of OP in AChE -/- mice was the same as in mice that had AChE, namely accumulation of excess acetylcholine followed by overstimulation of receptors. This leads to the conclusion that the physiologically important target of acute OP toxicity in AChE -/- mice is butyrylcholinesterase. Muscarinic receptors were found to be drastically downregulated in AChE -/- mice. It is possible that interaction of OP with muscarinic receptors also has a role in OP toxicity. These results predict that people with AChE deficiency will be unusually sensitive to OP toxicity, and will have abnormal reactions to muscarinic receptor drugs.

Introduction. The biochemical event that triggers convulsions and death after exposure to organophosphorus agents is inhibition of acetylcholinesterase. When AChE is inhibited, excess acetylcholine overstimulates acetylcholine receptors. This starts a cascade of neuronal excitation involving the glutamate receptors and excessive influx of calcium ions, that is responsible for the onset and maintenance of seizure activity [McDonough & Shih, 1997]. Inhibition of AChE has been documented in thousands of papers, and is the gold standard for measuring exposure to OP. This understanding of the mechanism of OP toxicity has led to effective therapies against OP poisons. Administration of atropine to block muscarinic receptors, of 2-PAM to reactivate AChE, and of anticonvulsant drugs, is standard clinical practice for treatment of OP toxicity. In view of the overwhelming evidence for a critical role for AChE in OP toxicity, it was of interest to determine the response of a mouse that had no AChE. If AChE were the only important target of OP, then mice with no AChE were expected to be resistant to OP toxicity.

Methods

Mice. AChE knockout mice were made by gene-targeting [Xie et al., 2000]. 5 kb of the AChE gene including the signal peptide, the catalytic triad, and 93% of the coding sequence were deleted. No AChE protein is made, and no AChE activity is present in any tissue. Since AChE -/- mice do not breed, the knockout colony is maintained by breeding heterozygotes. Pups in each litter are genotyped by PCR. The animals are in a strain 129Sv genetic background, produced by mating the

chimera (originating from R1 embryonic stem cells) to strain 129Sv mice (Taconic 129S6/SvEvTac). The AChE $-/-$ mice require special care and feeding as described by Duysen et al. [2002b] to enable them to live to an average of 100 days.

Organophosphorus agents and dose.

The nerve agent O-ethyl S-[2-(diisopropylamino)ethyl] methylphosphonothioate (VX) was from the Edgewood Chemical Biological Center (Aberdeen Proving Ground, MD). Animals were shipped to the U.S. Army Institute of Chemical Defense, Aberdeen Proving Ground, for experiments with VX. Tetraisopropyl pyrophosphoramidate (iso-OMPA) and diisopropylfluorophosphate (DFP) were from Sigma (St. Louis, MO). Chlorpyrifos oxon (CPO) was from Chem Service, Inc (West Chester, PA).

VX was dissolved in sterile saline and injected subcutaneously in the back of the neck at a dose of 8.0 – 25.0 $\mu\text{g/kg}$. Male and female animals were 34-55 days old. The number of animals for LD₅₀ experiments was $n = 21$ AChE $+/+$, $n = 18$ AChE $+/-$, $n = 16$ AChE $-/-$.

DFP was dissolved in sterile phosphate buffered saline and injected intraperitoneally at a dose of 2.5 mg/kg. Male and female animals were 12 days old. The number of animals was $n = 8$ AChE $+/+$, $n = 15$ AChE $+/-$, $n = 3$ AChE $-/-$.

Chlorpyrifos oxon was dissolved in dimethylsulfoxide and injected intraperitoneally at a dose of 0.1 to 4.0 mg/kg. Male animals were 49-200 days old. The number of animals was $n = 13$ AChE $+/+$, $n = 9$ AChE $-/-$.

Iso-OMPA was dissolved in sterile water and injected intraperitoneally at a dose of 1 – 550 mg/kg. Female mice were

90-210 days old. The number of animals was $n = 21$ AChE $+/+$, $n = 42$ AChE $+/-$, $n = 11$ AChE $-/-$.

Tissue extraction. Tissues were collected at time of death or 6 h after treatment, and frozen. Age and sex matched untreated control tissues were collected and stored in the same manner as the treated samples. Tissues were homogenized in 10 volumes of 50 mM potassium phosphate, pH 7.4, containing 0.5% Tween 20, in a Tisumizer (Tekmar, Cincinnati, OH) for 10 seconds. The suspension was centrifuged in a microfuge for 10 min, and the supernatant was saved for enzyme activity assays. The extraction buffer contained Tween 20 rather than Triton X-100 because mouse BChE activity was inhibited up to 95% by 0.5% Triton X-100, but was not inhibited by 0.5% Tween 20 [Li et al., 2000].

Enzyme activity assays in tissue

extracts. AChE and BChE activity was measured by the method of Ellman et al. [1961] at 25°C, in a Gilford spectrophotometer interfaced to MacLab 200 (ADInstruments Pty Ltd., Castle Hill, Australia) and a Macintosh computer. Samples were preincubated with 5,5-dithio-bis (2-nitrobenzoic acid) in 0.1 M potassium phosphate buffer, pH 7.0, to react free sulfhydryl groups before addition of substrate. AChE activity in tissues from VX treated animals was measured with 1 mM acetylthiocholine after inhibiting BChE activity with 0.1 mM iso-OMPA (liver required 1 mM for complete BChE inhibition). AChE activity in tissues from iso-OMPA treated mice was measured with 1 mM acetylthiocholine after inhibiting BChE with 0.01 mM ethopropazine. BChE activity was measured with 1 mM butyrylthiocholine.

Acylpeptide hydrolase activity was measured in tissues from VX treated mice in a SpectraMax 190 microtiter plate reader (Molecular Devices, Sunnyvale, CA). N-Acetyl-L-alanine p-nitroanilide (Sigma) was dissolved in 0.1 M Bis-Tris, pH 7.4, to make a 4 mM solution. The rate of hydrolysis of 4 mM N-acetyl-L-alanine p-nitroanilide was measured at 405 nm at 25°C. Each 200 µl of assay solution contained 5 µl of tissue extract. Absorbance was read every 5 min up to 40 min. Duysen et al. [2001] reported the results as ΔA_{405} per minute in a previous publication, but as µmoles per min per gram wet weight in Table 2.3 of the present report.

Units of activity for AChE, BChE and acylpeptide hydrolase are defined as µmoles substrate hydrolyzed per minute. Units of activity were calculated per gram wet weight of tissue.

Observations of OP treated animals.

Mice treated with organophosphorus toxicant (OP) were monitored up to 24 hours. Observations included salivation, lacrimation, increased urination, abnormal defecation, hyperactivity or lethargy, tremor, convulsions, muscle weakness, vasodilation. Body temperature was measured with a digital thermometer using a surface microprobe.

Muscarinic receptors measured by binding of 3H-QNB. 3H-quinuclidinyl benzilate (3H-QNB, New England Nuclear) is a nonselective muscarinic antagonist, which labels all five muscarinic receptor subtypes. Plasma membrane from mouse brains was prepared by homogenizing the tissue in a Dounce homogenizer in 10 volumes of ice-cold 50 mM TrisCl pH 8.0, containing 0.32 M

sucrose and protease inhibitor cocktail (Roche). The homogenate was centrifuged 10 min at 1000 x g. The pellet was discarded and the supernatant was centrifuged at 17,000 x g for 55 min; the membrane pellet was suspended in 2 ml of 50 mM Tris buffer pH 7.4. Protein concentrations were determined by the BCA protein assay (Pierce Chemical Co.). Membrane fractions containing 100 µg protein were mixed with 2 ml of 50 mM potassium phosphate buffer pH 7.4, containing a saturating concentration of 3H-QNB (3 nM). The mixture was incubated for 1.5 hours at room temperature. Nonspecific binding was determined in the presence of 10 µM atropine. The reactions were terminated by addition of 3 ml of ice-cold 50 mM potassium phosphate pH 7.4 and filtration under vacuum through Whatman GF/B glass fiber filter. The filters were washed three times with 3 ml of ice-cold 50 mM potassium phosphate buffer, then placed in 7 ml plastic minivials and dried. After addition of 4 ml EcoLume scintillation cocktail, radioactivity was measured in a Beckman liquid scintillation counter.

Behavioral measure of functional muscarinic receptors. Mice were injected subcutaneously with 0.2 mg/kg of the nonselective muscarinic receptor agonist oxotremorine. Body temperature was assessed immediately before and after injection. Body temperature was measured with a surface thermometer (Thermalert model TH-5 and a surface Microprobe MT-D, type T thermocouple, Physitemp Instruments Inc., Clifton, N.J.).

Results

Phenotype of the adult AChE $-/-$ mouse.

Adult AChE $-/-$ mice are not normal in appearance. When they walk, the tail and abdomen drag on the ground. Their feet splay out and their gait is abnormal. They have no grip strength. By one year of age, AChE $-/-$ mice never stand on their hind legs and they do not climb. They have a hump in their back, suggesting a deformed skeleton. They do not eat solid food, and cannot lift the head to drink from a suspended bottle. Body tremor is noticeable when they are moving about, but not when they are asleep. They have pinpoint pupils.

They are lethargic, spending most of the time hiding in a small dark box inside their cage. Another behavioral abnormality is their lack of housekeeping behavior; they defecate and urinate in their nest. They do not engage in mating behavior. AChE $-/-$ mice have never become pregnant despite being housed all their life with male AChE $-/-$ mice ($n=600$).

About 25% of adult AChE $-/-$ mice make a bird-like chattering sound when they are disturbed. This vocalization is a response to stress.

Adult female AChE $-/-$ mice are small, averaging 18 g. In contrast, wild-type female littermates weigh 27-32 g. A few male AChE $-/-$ mice reach a weight of 30-35 g, though the average male knockout mouse weighs 18 g. The surface body temperature of adult AChE $-/-$ mice is 36.5°C, while that of AChE $+/+$ mice is 37.1°C.

The average lifespan of AChE $-/-$ mice is 100 days, though several have lived a normal lifespan of 2 years. In contrast, AChE $+/+$ mice live for 2 years. AChE $-/-$ mice die of stress-induced seizures. A

disproportionate number of AChE $-/-$ mice die on postnatal days 30-40. More details on the phenotype of adult AChE $-/-$ mice are in Duysen et al. [2002b].

Phenotype of AChE $+/-$ mice.

Heterozygous mice, carrying one deficient AChE allele, and expressing 50% of the normal AChE activity in tissues [Xie et al., 2000; Li et al., 2000], are indistinguishable from wild-type mice in appearance. They have a normal lifespan, are sexually active, and fertile. Their litter sizes are the normal 6-8 pups. A female AChE $+/-$ mouse has an average of 6-8 litters in her lifetime, similar to the number of litters produced by an AChE $+/+$ mouse of strain 129Sv. No health problems have been noticed in AChE $+/-$ mice. They do not have seizures.

The observation that mice with 50% of normal AChE activity are healthy supports the idea that the amount of AChE in tissues is in excess of what is needed. In view of this, it was surprising to find that AChE $+/-$ mice have a reduced number of functional muscarinic receptors.

Muscarinic receptors. Functional muscarinic receptors were quantitated in two ways: by binding of the radioligand 3H-QNB, and by behavioral assays measuring the response to the muscarinic agonist oxotremorine. Figure 2.1 shows that plasma membrane from AChE $-/-$ brain bound about 50% of the 3H-QNB compared to AChE $+/+$, suggesting a 50% reduction in muscarinic receptors in AChE $-/-$ mouse brains. The heterozygous AChE $+/-$ mouse had an intermediate binding capacity, suggesting that brains of AChE $+/-$ mice also had reduced numbers of muscarinic receptors.

Wild-type AChE $+/+$ mice treated with the muscarinic agonist oxotremorine at a dose of 0.2 mg/kg lost 8°C of body

temperature within 30 minutes. The temperature remained at a low 29°C for 40 minutes, slowly returning to normal in 3 hours (Figure 2.2). Heterozygous AChE +/- mice also lost body temperature, dropping 6°C; they regained their normal body temperature of 37.1°C after 2 hours. In contrast, AChE -/- mice showed no response at all to 0.2 mg/kg oxotremorine. Their body temperature remained normal.

These results support the conclusion that AChE -/- mice have dramatically reduced numbers of functional muscarinic receptors, and that AChE +/- mice also have reduced numbers of functional muscarinic receptors. The number of functional muscarinic receptors in AChE +/- mice appears to be intermediate to that in knockout and wild-type mice.

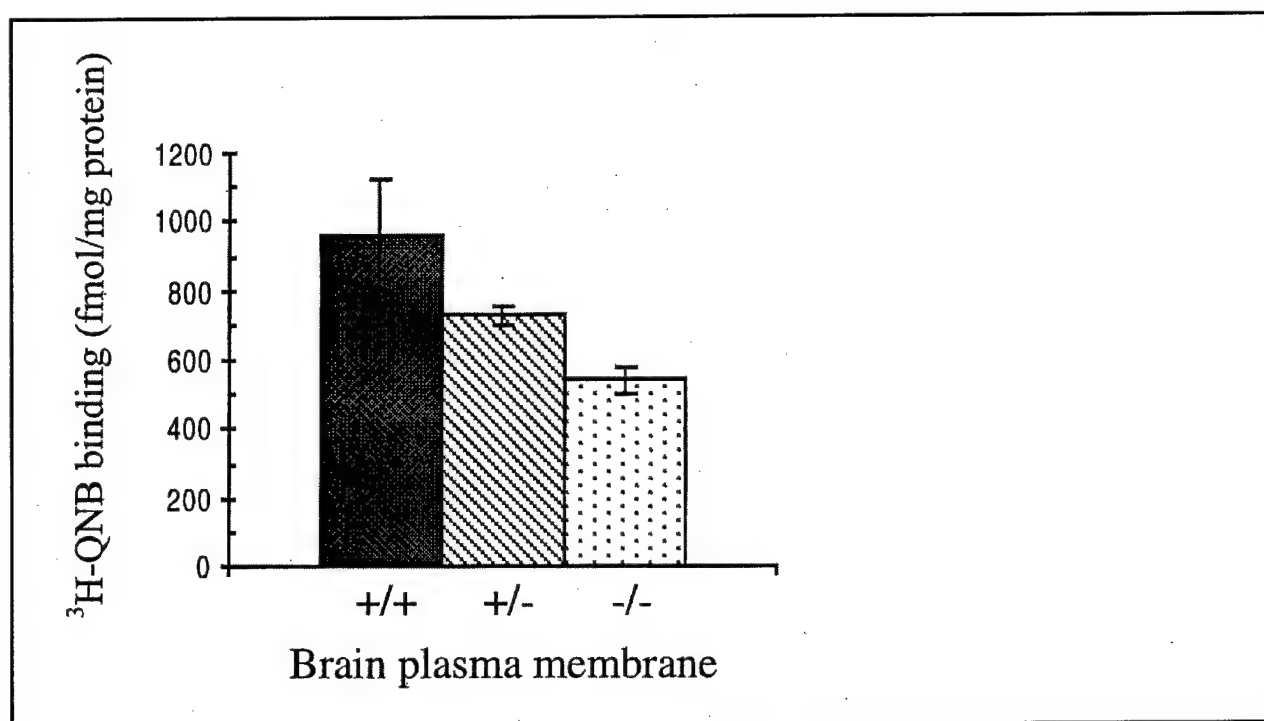


Figure 2.1. Muscarinic receptor density in mouse brains. Brain membranes from AChE +/+, +/-, and -/- mice (n =3 for each group) were tested for muscarinic receptor density by binding of the radioligand 3H-QNB at a saturating concentration of 3 nM. Data are the mean \pm S.E.

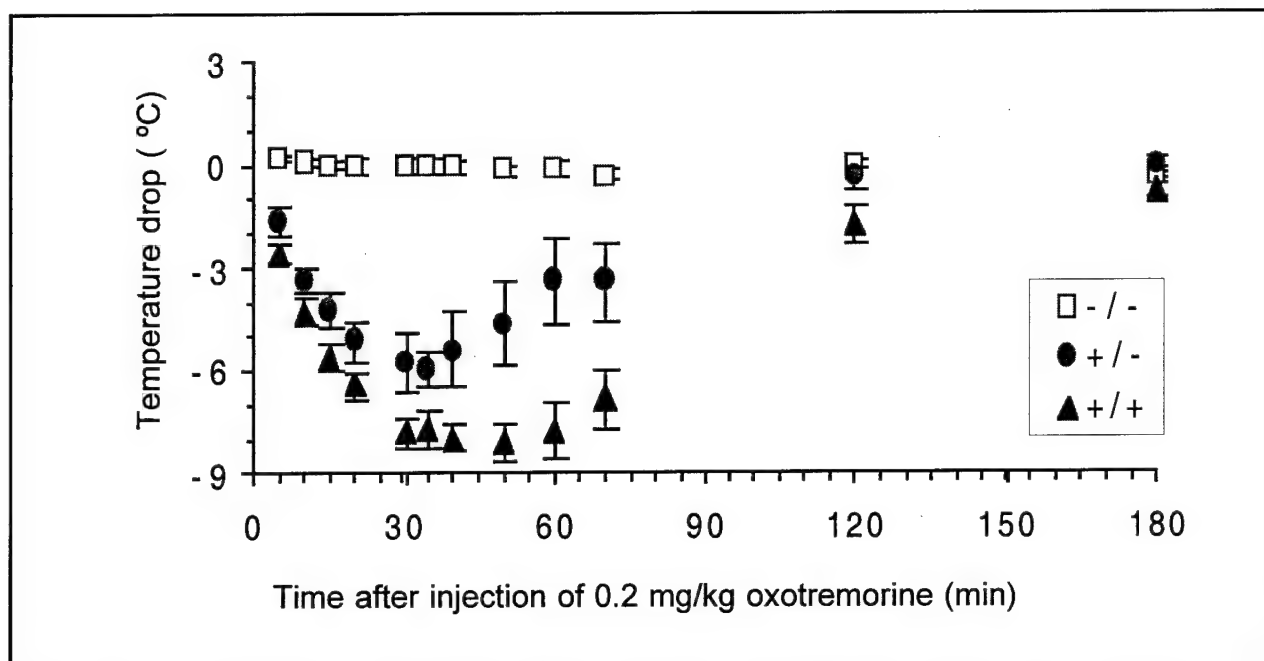


Figure 2.2. Behavioral response of live mice to oxotremorine. Mice (n =6 in each group) were injected subcutaneously with 0.2 mg/kg oxotremorine. Surface body temperature was measured. This shows that AChE $-/-$ mice are resistant to oxotremorine. It is concluded that AChE $-/-$ mice have fewer functional muscarinic receptors.

LD₅₀ of OP. Strain 129Sv mice, differing only at the AChE gene locus, were tested with four organophosphorus toxicants (Table 2.1). Mice with no AChE were supersensitive to the lethal effects of DFP, chlorpyrifos oxon, VX, and iso-OMPA. Iso-OMPA discriminated between AChE $-/-$ and $+/+$ mice more effectively than the other OP. A dose of 1 mg/kg was lethal to half of the AChE $-/-$ mice but produced

no toxic symptoms in AChE $+/+$ and $+/-$ mice. The dose had to be increased 350-fold before iso-OMPA was lethal to AChE $+/+$ and $+/-$ animals. The nerve agent VX is the most potent OP known. Microgram quantities are lethal. The finding that AChE $-/-$ mice succumbed to VX shows that VX reacts with targets other than AChE and that reaction results in death.

Table 2.1. LD₅₀ of organophosphorus toxicants in wild-type and AChE deficient mice, strain 129Sv.

AChE Genotype	AChE activity	DFP LD ₅₀	Chlorpyrifos Oxon LD ₅₀	VX LD ₅₀	Iso-OMPA LD ₅₀
AChE $+/+$	100%	> 2.5 mg/kg	3.5 mg/kg	24 µg/kg	350 mg/kg
AChE $+/-$	50%	2.5 mg/kg	-	17 µg/kg	350 mg/kg
AChE $-/-$	0 %	< 2.5 mg/kg	0.5 mg/kg	11 µg/kg	1 mg/kg

Symptoms of toxicity after OP treatment.

Untreated AChE $-/-$ mice have cholinergic symptoms of OP toxicity even though they have never received any OP. Whole body tremor, pinpoint pupils, mucus on the eyes, and reduced body temperature are characteristic of untreated AChE $-/-$ mice and are also cholinergic signs of toxicity attributed to excess acetylcholine.

Treatment with a nonlethal dose of VX caused a hypothermic response reminiscent of the response to oxotremorine. AChE $-/-$ mice were resistant to the hypothermic effects of VX, whereas AChE $+/+$ mice lost 8°C of surface body temperature and did not regain normal temperature for 24 hours [Duysen et al., 2001]. The resistance of AChE $-/-$ mice to the hypothermic effects of VX can be explained by a reduced number of functional M2 muscarinic receptors. The receptors involved in thermal regulation are M2 [Gomez et al., 1999].

Since the signs of OP toxicity are attributed to inhibition of AChE, it was of interest to determine whether mice with no AChE activity had different symptoms. Table 2.2 summarizes the symptoms observed in response to lethal injections of 4 different OP. AChE $-/-$ mice exhibited the same symptoms as wild-type and heterozygous mice. Exceptions to this pattern are the salivation observed in iso-OMPA treated AChE $-/-$ mice and the absence of hyperactivity in DFP treated AChE $-/-$ mice. The lack of hyperactivity in DFP treated AChE $-/-$ mice is explained by the fact that they died instantly, before movement could be observed.

The pattern of symptoms was different for each OP. This observation has been taken as evidence that OP react with several targets, and that the toxicity is not explained by inhibition of AChE alone [Pope et al., 1999; Moser 1995].

Table 2.2. Toxic signs in OP treated AChE $+/+$, $+/-$, and $-/-$ mice, following a lethal dose of OP.

OP	AChE genotype	Salivation	Mucus in eyes	Urination	Defecation	Reduced body temp	hyperactivity	tremor (clonic or tonic)	Convulsions	Vasodilation
CPO	$+/+$	no	yes	no	no	yes	no	yes	yes	yes
CPO	$-/-$	no	yes	no	no	yes	no	yes	yes	yes
VX	$+/+$	yes	yes	no	no	yes	no	yes	yes	yes
VX	$+/-$	yes	yes	no	no	yes	no	yes	yes	yes
VX	$-/-$	yes	yes	no	no	yes	no	yes	yes	yes
iso-OMPA	$+/+$	no	yes	no	yes	yes	yes	yes	no	no
iso-OMPA	$+/-$	no	yes	no	yes	yes	yes	yes	no	no
iso-OMPA	$-/-$	yes	yes	no	no	yes	yes	yes	no	no
DFP	$+/+$	yes	-	yes	no	yes	yes	yes	-	-
DFP	$+/-$	yes	-	yes	no	yes	yes	yes	-	-
DFP	$-/-$	yes	-	yes	no	yes	no	yes	-	-

CPO is chlorpyrifos oxon.

Enzyme activity in tissues. This work is ongoing and is not yet complete. Tissues from VX treated animals [Duysen et al., 2001] and a few tissues from iso-OMPA treated animals have been tested. The results in Table 3.3 show that a lethal dose of VX inhibited AChE in brain 50%. BChE in brain was also inhibited about 50%. The extent of BChE inhibition in AChE -/- brain was no greater than in AChE +/+ and +/- brains. Similarly, AChE in muscle and serum was also inhibited about 50%, whereas AChE in intestine showed almost no inhibition. BChE activity was inhibited in all tissues tested.

Acylpeptide hydrolase was not significantly inhibited by VX (Table 2.3). Acylpeptide hydrolase was of interest because Richards et al. [2000] found that acylpeptide hydrolase was inhibited by doses of dichlorvos, chlorpyrifos methyl oxon, and diisopropylfluorophosphate that did not inhibit AChE. It was unknown whether

acylpeptide hydrolase would be preferentially inhibited by VX. Our results lead to the conclusion that acylpeptide hydrolase is not a major target of VX and that inhibition of acylpeptide hydrolase does not explain the supersensitivity of AChE-/- mice to VX.

A dose of 5 mg/kg iso-OMPA had no toxic effects on AChE +/+ and +/- mice, but was lethal to AChE -/- mice. Iso-OMPA is regarded as a specific inhibitor of BChE, however AChE activity in serum and liver was inhibited 50% and 95% respectively. BChE activity was inhibited in brain, serum and liver. The BChE activity in AChE -/- mice was almost totally inhibited by this dose of iso-OMPA when the BChE tested was in peripheral tissues. Brain BChE was less inhibited, suggesting that iso-OMPA does not readily cross the blood brain barrier.

Table 2.3. AChE, BChE, and acylpeptide hydrolase activity in tissues of mice treated with a lethal dose of VX. Units of enzyme activity are μ moles substrate hydrolyzed per min per gram wet weight of tissue. The standard deviations were 3 to 30% of the average values shown.

Genotype	Tissue	AChE		BChE		Acylpeptide Hydrolase	
		Control	VX	Control	VX	Control	VX
+/+	brain	1.71	0.86 ^a	0.13	0.05 ^a	0.10	0.10
+/-	brain	0.91	0.53 ^a	0.11	0.05 ^a	0.11	0.11
-/-	brain	0	0	0.10	0.05 ^a	0.11	0.10
+/+	muscle	0.28	0.15 ^a	0.26	0.14	0.10	0.10
+/-	muscle	0.22	0.11 ^a	0.25	0.11 ^a	0.16	0.11
-/-	muscle	0	0	0.27	0.11 ^a	0.11	0.11
+/+	intestine	0.21	0.20	5.97	5.08	0.31	0.22
+/-	intestine	0.15	0.14	4.37	3.77	0.31	0.26
-/-	intestine	0	0	7.95	6.28	0.32	0.28
+/+	serum	0.54	0.31 ^a	2.79	1.64	ND ^b	ND
+/-	serum	0.28	0.21	1.75	1.14 ^a	ND	ND
-/-	serum	0	0	1.88	1.48	ND	ND

^a significantly different from control $p \leq 0.025$ by ANOVA using Bonferroni correction to adjust for multiple comparisons.

^bND, not determined

Discussion

Why is the acetylcholinesterase knockout mouse supersensitive to organophosphorus agent (OP) toxicity?

The goal of this work was to find out why the acetylcholinesterase knockout mouse was supersensitive to OP toxicity. Since this mouse has zero AChE activity, it must be concluded that OP inhibited enzymes other than AChE and that the consequence of this inhibition was lethal to the AChE $-/-$ mouse.

Our results suggest that inhibition of BChE is part of the explanation for the lethality of OP in AChE knockout mice. Another part of the explanation may involve the drastically reduced muscarinic acetylcholine receptor levels.

Evidence to support the idea that BChE inhibition is lethal to AChE $-/-$ mice includes the following. 1) BChE was inhibited in OP treated AChE $-/-$ mice. 2) AChE $-/-$ mice had the same cholinergic signs of toxicity following treatment with OP, as AChE $+/+$ mice. This means the mechanism of toxicity was the same, even though AChE $-/-$ mice have no AChE. The common mechanism would be accumulation of excess acetylcholine, followed by overstimulation of acetylcholine receptors. Inhibition of BChE could lead to accumulation of excess acetylcholine, because BChE is capable of hydrolyzing acetylcholine. The implication in this conclusion is that BChE has a function in AChE $-/-$ mice to hydrolyze the neurotransmitter acetylcholine at cholinergic synapses. Mesulam et al. [2002] proposed such a function for BChE in brain.

An additional experiment that is planned for the future is to measure acetylcholine levels in the brains of AChE $-/-$ mice before and after OP treatment.

If it were found that acetylcholine concentration increased after OP treatment, then the mechanism of toxicity of OP in AChE $-/-$ mice would implicate BChE. Based on the data presently available, we conclude that the acute toxicity of OP in AChE knockout mice is due to inhibition of BChE.

Muscarinic receptors. The reduced numbers of functional muscarinic acetylcholine receptors (and presumably nicotinic acetylcholine receptors) in AChE deficient mice complicates the interpretation. OP can covalently bind to muscarinic receptors [Bomser & Casida, 2001] and interfere with signal transduction [Huff et al., 1994]. The already low levels of functional muscarinic receptors in the knockout mice could be further reduced by binding of OP, leading to a level that is lethal. This would mean that a combination of receptor malfunction and BChE inhibition would explain supersensitivity to OP.

Implications for man. Humans with muscle end-plate AChE deficiency have been identified [Donger et al., 1998; Ohno et al., 1998]. Their AChE deficiency is explained by mutations in the COLQ gene. The mutations make it impossible to anchor the AChE protein via a collagen tail to the neuromuscular junction [Feng et al., 1999]. No cases of AChE deficiency due to mutations in the human AChE gene have been found as of the year 2002. Our finding that heterozygous mice who carry one deficient AChE allele are healthy, suggests that in the future we will find healthy humans who carry one deficient AChE allele. These humans will be more sensitive to OP toxicity than the average

person, and in addition, they will have an abnormal reaction to drugs targeted at muscarinic acetylcholine receptors.

Summary of results for Task 2.

- A method was developed for prolonging the life of AChE knockout mice to adulthood. Previously they had died at 12 days, but with special feeding they now live to 100 days or even to 2 years.
- AChE $-/-$ mice were supersensitive to all OP tested including DFP, the nerve agent VX, chlorpyrifos oxon, and iso-OMPA.
- A dose of iso-OMPA that had no toxic effects on wild-type mice, was lethal to AChE $-/-$ mice.
- Muscarinic acetylcholine receptors were drastically reduced in AChE $-/-$ mice.
- Treatment with OP caused the same cholinergic signs of toxicity in wild-type and AChE deficient mice. This was a surprising result because cholinergic signs are attributed to inhibition of AChE, yet AChE $-/-$ mice have no AChE.
- Mice with 50% of normal AChE activity were healthy. They differed from wild-type mice in two respects: they were more sensitive to OP toxicity, and they had reduced numbers of muscarinic receptors.
- The acute toxicity of OP in AChE knockout mice is due to inhibition of BChE. The drastically reduced muscarinic acetylcholine receptor levels may also have a role in the supersensitivity of AChE knockout mice to OP.

Task 3.

Human and mouse brains will be extracted and treated with biotinylated OP. The biotinylated proteins will be purified with avidin-Sepharose, and separated by gel electrophoresis. The number and size of proteins that reacted with biotinylated OP will be visualized on blots by treating with avidin conjugated to an indicator.

Progress on Task 3 is described in the following section. All work to date has been with mouse brain extracts.

Abstract. A method was developed that will ultimately lead to identification of biological markers of low dose exposure to OP. In the new method proteins are labeled with biotinylated-OP, separated on SDS-PAGE, transferred to a membrane, and visualized with StreptAvidin-conjugated to a fluorophore. Fluorescence is detected with an Infrared Imaging System. Reproducible patterns are obtained that allow quantitation of band intensities. This method allows us to progress to Task 5, where we begin to measure the reactivity of 29 proteins with various insecticides.

Introduction. Existing methods were insufficient to allow broad range screening of OP reactivity. Therefore, we developed a new method and used a new detection strategy to increase sensitivity, maintain good resolution, and improve reproducibility.

Methods

Preparation of sub-cellular fractions from mouse brain, and protein

quantitation. Mouse brain was separated into its sub-cellular fractions by centrifugation, essentially as described by Gray and Whittaker [1962]. Brain tissue was homogenized by two 1-minute disruptions with a Potter-Elvehjem homogenizer (Teflon pestle with glass vessel) rotating at 840 rpm (in 10-volumes of ice cold 50 mM Tris/Cl buffer, pH 8.0, containing 0.32 M sucrose, to prevent disruption of organelles). The suspension was centrifuged at 1000xg for 10 minutes at 4°C to pellet nuclei, mitochondria, plasma membranes and unbroken cells. The supernatant was re-centrifuged at 17,000xg for 55 minutes at 4°C to pellet myelin, synaptosomes and mitochondria. That supernatant was re-centrifuged at 100,000xg for 60 minutes at 4°C to separate microsomes (pellet) from soluble proteins (supernatant).

Protein in the supernatant fraction was estimated by absorbance at 280 nm, using $A_{280} = 1.0$ for 1 mg protein/ml. The 100,000xg supernatant was divided into 0.4 ml aliquots and stored at -70°C, along with the other sub-cellular fractions.

Initial screening protocol. A process for screening brain extracts for organophosphate-reactive proteins involved the following ten steps:

- 1) Treat the brain extracts, for a defined time, with various concentrations of the organophosphate of interest.
- 2) Separate the proteins from excess organophosphate by gel filtration,

- using a spin-column.
- 3) React the treated extracts with FP-biotin to label all remaining organophosphate reactive proteins.
 - 4) Purify the biotinylated proteins using Avidin-Sepharose.
 - 5) Separate the purified, biotin-containing proteins on SDS-PAGE.
 - 6) Transfer the proteins to a membrane.
 - 7) Block the membrane and treat with avidin, conjugated to horseradish peroxidase.
 - 8) Treat the avidin-horseradish peroxidase labeled membranes with a chemiluminescent reagent and detect the emitted light on x-ray film.
 - 9) Quantitate the emitted light, which is directly proportional to the level of biotin, densitometrically.
 - 10) Analyze the densitometer signal intensities to obtain second-order rate constants for the reactions of the organophosphates of interest with each of the organophosphate-reactive proteins in the brain extract.

Steps 3 to 9 in this process were based on protocols reported by Cravatt and co-workers [Liu et al., 1999; and Kidd et al., 2001]. The concept for determination of second-order rate constants was adopted from Richards et al., [1999]. Our initial trials employed the following conditions for steps 3 to 9 and reflect the conditions of Cravatt and co-workers:

- 3) Reaction with FP-biotin. Mouse brain supernatant (100,000xg) at 1 mg protein/ml was reacted with 2 μ M FP-biotin in 0.1 M Tris/Cl buffer pH 8.0 at 25°C for 30 minutes. Reactions were stopped by the addition of 1/5 volume of 0.2 M Tris/Cl buffer, pH 6.8, containing 10% SDS, 30% glycerol, 0.6 M dithiothreitol and 0.012% bromophenol blue; followed by incubation at 80°C for 5 minutes.

- 4) SDS-PAGE. From 10-50 μ g of protein were applied per lane to a 4-30% SDS PAGE, with 4% stacking gel, and run for 3000 volt-hours at room temperature. The bottom tank buffer consisted of 60 mM Tris/Cl buffer, pH 8.1, plus 0.1% SDS. The top tank buffer consisted of 25 mM Tris/192 mM glycine buffer, pH 8.2, plus 0.1% SDS. This is essentially the same as the Laemmli protocol [1970].
- 5) Transfer from gel to membrane. Protein was transferred to PVDF membrane (ImmunBlot from BioRad) in 25 mM Tris/192 mM glycine buffer, pH 8.2, using a tank system (TransBlot from BioRad), for 1 hour, at 0.5 amps, in the cold room.
- 6) Blocking and labeling. Membranes were blocked with 3% nonfat dry milk in Tris-buffered-saline plus 1% Tween-20, labeled with avidin-horseradish peroxidase (at 9.7 nM avidin, from BioRad), and washed with Tris-buffered-saline as described by Liu et al., [1999].
- 7) Biotin labeling and signal detection. Membranes were treated with chemiluminescent reagents (LumiGLO from Kirkegaard & Perry) according to the manufacture's instructions. Light emission was detected with x-ray film.
- 8) Signal measurement. Signal intensity was measured densitometrically using the Kodak EDAS 120 image analysis system.
- 9) Signal quantitation. Signal intensities were quantitated with Kodak 1D software using a Gaussian deconvolution algorithm.

Results similar to those reported by Liu et al., [1999] were obtained, but it soon became apparent that this protocol would have to be refined in order to suit our purposes.

Refinement of the screening protocol.

The changes which were made, and the reasons for those changes are described below:

Reaction conditions: When the time courses for reaction of 2 μ M FP-biotin with the organophosphate-reactive proteins in mouse brain supernatant were examined, none of the reactions approached completion by 30 minutes. A reliable reaction end-point is essential for the accurate determination of the reaction kinetics. In order to obtain complete reaction time courses, concentrations of FP-biotin up to 40 μ M and reaction times out to 450 minutes were ultimately used.

With such prolonged reaction times, complications from proteolysis became of concern. Five millimolar EDTA was added to the reaction mixture in order to reduce the possibility of proteolysis. However, no evidence of proteolysis ever appeared. This statement is based on the following observations. First, the signals from the two major, endogenous, biotinylated proteins remained constant throughout the reaction time course (to within experimental limits). Second, rapidly reacting proteins reached maximum signal intensity quickly and maintained that signal level throughout the remainder of the incubation.

Methanol (2.4%) was added to the reaction mixture to accommodate the introduction of methanol along with the higher levels of FP-biotin.

Purification of the biotin-labeled proteins: Attempts to purify the FP-biotin labeled proteins by extraction with avidin-Agarose (Sigma) revealed that many proteins were resistant to extraction. Pre-treatment with SDS (0.5%) and heat, as described by Kidd [2001] improved the

extraction, but extraction of many proteins remained incomplete. This step promised to introduce an unacceptable level of error for kinetic purposes, so it was dropped from the screening protocol. Purification by avidin-Agarose extraction will be used eventually, to prepare biotin-labeled proteins for identification.

SDS-PAGE: When reactions were performed with higher FP-biotin concentrations and for longer times, more proteins were labeled. Since it is not clear which proteins might prove important in low level exposure to some organophosphates, it was decided to screen as many organophosphate-reactive proteins as possible. For this purpose, the best possible resolution on the SDS-PAGE was desirable. Toward that end, gradient gels were tested at 4-30%, 4-10%, 10-20%, and 20-30%; in addition, fixed concentration gels were tested at 10%, 15%, and 20%, all with 4% stacking gels. The 10-20% gradient gel gave the best resolution. Running the gel in the cold room (at 4°C), with stirring of the bottom buffer, improved the quality of the bands. It was found that using a 10-20% gradient, with a 4% stacking gel, at 4°C, for 3000 volt-hours spread the proteins over 80% of the separating gel height.

Electroblotting: FP-biotin reactive proteins were found to cover a wide range of molecular weights (15 to 100 kDa), and many proteins were clustered in overlapping groups. In order to optimize transfer from gel to membrane for all of the proteins, and to maximize the resolution of the transferred bands, various conditions for transfer were tested. PVDF membrane was chosen over nitrocellulose because it is easier to handle. ImmunBlot membrane (BioRad)

was used because it has a high internal surface area, capable of trapping large amounts of protein (140-150 μg protein/ cm^2). Under our transfer conditions, a single layer of ImmunBlot trapped all of the protein transferred from a gel containing mouse brain supernatant; no protein passed through the membrane. Electrophoretic transfer using a tank with plate electrodes (TransBlot from BioRad) was employed. The transfer buffer consisted of 25 mM Tris/192 mM glycine, pH 8.2. Addition of 10% methanol or 0.005% SDS made no obvious improvement to overall transfer. Addition of 0.05% SDS decreased transfer efficiency. Transfer was made using 0.5 amps, for 1 hour, in the cold room (4°C), with stirring. Gels stained with Coomassie Blue after the tank transfer showed little or no residual protein.

Semi-dry transfer was tested with both the BioRad TransBlot SD and Millipore Graphite ElectroBlotter II, using the manufactures recommended protocols. The protein bands transferred by the semi-dry method were not as well resolved as those from the tank transfer, and not as much protein was transferred.

Blocking, labeling and washing of membranes: The protocol of Liu et al., [1999] (blocking with 3% nonfat dry milk and 1% Tween-20 in Tris-buffered-saline; labeling in Tris-buffered-saline containing 1% Tween-20 and 1% nonfat dry milk; and washing with Tris-buffered-saline) was compared both to the protocol recommended by Amersham [Amershampharmaciabiotec, RPN 2106 PL/99/10] (blocking with 5% nonfat dry milk in 20 mM Tris/Cl buffer, pH 7.4, plus 150 mM NaCl and 0.2% Tween-20; labeling in 20 mM Tris/Cl buffer, pH 7.4, containing 150 mM NaCl, 0.2% Tween-20 and 5% nonfat dry milk; and extensive

washing with 20 mM Tris/Cl buffer, pH 7.4, containing various amounts of Tween-20 and nonfat dry milk), and the protocol recommended by BioRad [BioRad Lit 171 Rev D] (blocking with 3% gelatin in 20 mM Tris/Cl buffer, pH 7.5, containing 500 mM NaCl; labeling in 20 mM Tris/Cl buffer, pH 7.5, containing 500 mM NaCl, 1% gelatin, and 0.05 % Tween-20; and washing with 20 mM Tris/Cl buffer, pH 7.5, containing 500 mM NaCl \pm 0.05% Tween-20). The BioRad protocol yielded the lowest background signal and was adopted.

Labeling the biotin: The biotinylated proteins were initially labeled with an avidin-horseradish peroxidase conjugate (BioRad). The signals were detected using chemiluminescent reagents (LumiGLO from Kirkegaard & Perry) and x-ray film; then quantitated by densitometry from the film (Kodak EDAS 120). As the concentration of FP-biotin was increased and the reaction times were lengthened, it became apparent that the dynamic range of the film (typically 50-fold from weakest to strongest signal) was too small to serve the range of signals on the membrane, which were very weak for short-time reactions with proteins present in low amount to very strong for long-time reactions with proteins present in high amount.

The film was therefore replaced with a charge coupled device (CCD) digital camera, the LAS-1000 plus Luminescent Image Analyzer (FujiFilm). This device uses a cooled CCD camera to detect low level light emission and supports a 16-bit dynamic range (65,500-fold). The data can be transferred directly to the Kodak 1D analysis program (version 3.5.3 supports 16-bit data) thereby eliminating the densitometry step. However, this device does not deliver the resolution of x-ray film, because the camera needs to be about 2

feet from the film in order to capture the entire field. In addition, a collection time of 15 minutes is required to detect the weaker signals. Such a long data collection period results in a high background, and can lead to depletion of the chemiluminescent reagents in the vicinity of proteins present in high amounts. Data collection is further complicated by the fact that such long-time exposure to the chemiluminescence reagents (specifically the peroxide) causes irreversible inhibition of the horseradish peroxidase.

All of these difficulties were overcome when the Odyssey Infrared Imaging System (LI-COR) was purchased by the department. The Odyssey employs an infrared laser to excite a fluorescent probe, which is attached to the target protein; and then collects the emitted light. The emitted light intensity is directly proportional to the amount of probe. Both the laser and the detector are mounted on a moving carriage positioned directly below the membrane. The membrane can be scanned in step sizes as small as 21 microns, providing resolution comparable to x-ray film. Data are collected using a 16-bit dynamic range, and can be transferred directly to the Kodak 1D analysis program. The fluorophore is stable in the laser, making it possible to scan the membrane repeatedly, using different intensity settings to optimize data collection for both strong and weak signals. Membranes are now labeled with StreptAvidin conjugated to an Alexa-680 fluorophore (Molecular Probes) for use with the Odyssey.

Current protocol. Currently our protocol consists of eight steps. The first two steps: Reaction of the brain extracts with organophosphates of interest; and separation of the proteins from excess

organophosphate by gel filtration on a spin column, will be described in Task 5.

Step 3) Reaction with FP-biotin. Mouse brain supernatant (1.25 mg protein/ml) is reacted with 2-40 μ M FP-biotin in 50 mM Tris/Cl buffer, pH 8.0, containing 5 mM EDTA and 2.4% methanol at 25°C for up to 450 minutes. Reaction is stopped by addition of 1/5 volume of 10% SDS, 30% glycerol, 0.6 M dithiothreitol, and 0.012% bromophenol blue in 0.2 M Tris/Cl buffer, pH 6.8; followed by heating at 80°C for 5 minutes.

Step 4) SDS-PAGE. A 10-20% gradient PAGE with 4% stacking gel is used (overall dimensions are 16x18x0.075 cm, with 20 wells/lanes). Twenty-four micrograms of total protein are loaded per lane, and run for 3000 volt-hours in the cold room (4°C), with stirring. The bottom tank contains 60 mM Tris/Cl buffer, pH 8.1, plus 0.1% SDS. The top tank buffer contains 25 mM Tris/192 mM glycine buffer, pH 8.2, plus 0.1% SDS. Gels and buffers are prepared essentially as described by Laemmli [1970].

Step 5) Western Blotting. Protein is transferred from gel to PVDF membrane (ImmunBlot from BioRad) electrophoretically in a tank using plate electrodes (TransBlot from BioRad), at 0.5 amps, for 1 hour, using 25 mM Tris/192 mM glycine buffer, pH 8.2, in the cold room (4°C), with stirring.

Step 6) Blocking the membrane, labeling the biotin, and washing. The membrane is blocked with 3% gelatin (BioRad) in 20 mM Tris/Cl buffer, pH 7.5, containing 0.5 M NaCl for 1 hour at room temperature. Then it is washed twice with 20 mM Tris/Cl buffer, pH 7.5, containing 0.5 M NaCl and 0.05% Tween-20, for 20 minutes. Biotinylated proteins are labeled with 9.5 nM

Streptavidin-Alexa 680 conjugate (Molecular Probes) in 20 mM Tris/Cl buffer, pH 7.5, containing 0.5 M NaCl and 1% gelatin, for 2 hours, at room temperature, protected from light. Shorter reaction times resulted in less labeling. Then the membrane is washed twice with 20 mM Tris/Cl buffer, pH 7.5, containing 0.5 M NaCl and 0.05% Tween-20, and twice with 20 mM Tris/Cl buffer, pH 7.5, containing 0.5 M NaCl, for 20 minutes each. This is essentially the BioRad protocol [BioRad Lit 171 Rev D].

Step 7) Signal detection. Membranes are scanned with the Odyssey (LI-COR) at 42 microns per pixel.

Step 8) Signal intensity analysis. The intensity of the signal from each labeled protein is determined using a Gaussian deconvolution routine from the Kodak 1D Image Analysis program, v 3.5.3 (Kodak).

Results

With this protocol, 29 FP-biotin reactive proteins could be resolved reproducibly from the 100,000xg mouse brain supernatant. Figure 3.1 shows these 29 proteins plus the 3 endogenous, biotinylated proteins (bands 1, 7 and 8) for a total of 32 bands.

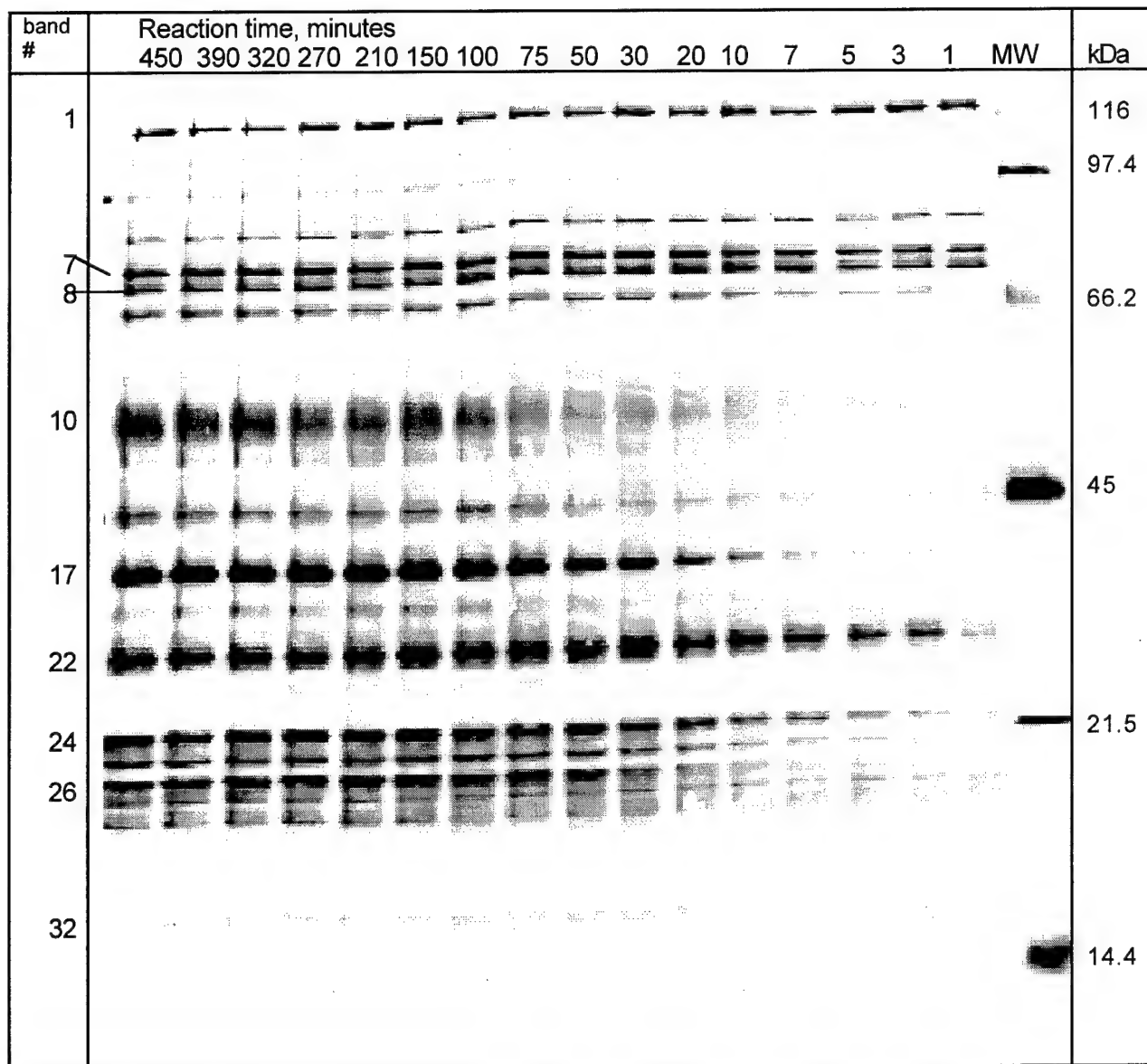


Figure 3.1. SDS-PAGE showing the time course for the reaction of FP-biotin with proteins extracted from mouse brain. The 10 μ M FP-biotin was reacted with 1.25 mg protein/ml of mouse brain supernatant in 50 mM Tris/Cl buffer, pH 8.0, containing 5 mM EDTA and 2.4% methanol, at 25°C, for selected times. The numbers above each lane indicate the reaction times in minutes. Biotinylated molecular weight markers (BioRad) are β -galactosidase (116 kDa), phosphorylase B (97.4 kDa), bovine serum albumin (66.2 kDa), ovalbumin (45 kDa), soybean trypsin inhibitor (21.5 kDa) and lysozyme (14.4 kDa). Endogenous biotinylated proteins are in bands 1, 7, and 8.

A single lane from Figure 3.1 is shown in Figure 3.2. The signal intensity in each band is represented as peaks. The numbers associated with each peak are the band numbers. For example, band 17 is the most intense band on the gel.

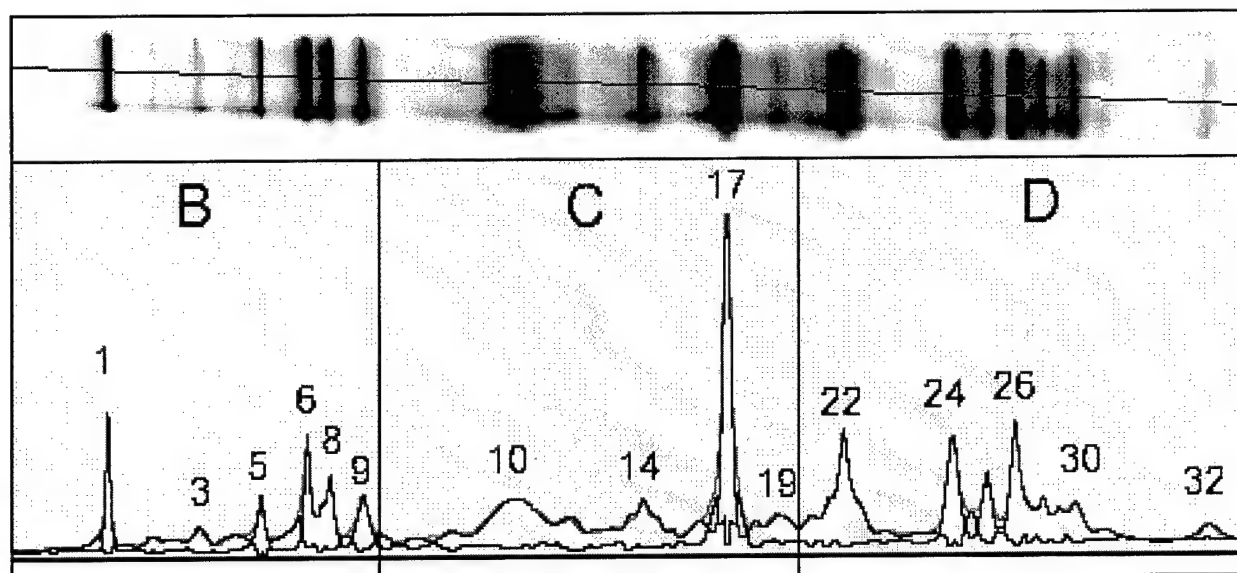


Figure 3.2. Biotinylated proteins from mouse brain supernatant. The upper portion is a picture of the fluorescence signals from the biotinylated proteins labeled in a 270 minute reaction with 10 μ M FP-biotin. The lower portion is a collection of traces describing the band pattern. There is a trace of the measured fluorescence intensity, which is overlaid by a trace of the fitted intensity obtained from a Gaussian deconvolution of the data. Below these traces is a trace of the difference between measured and fitted data. The numbers identify the individual bands. The vertical lines define the portions of this figure which are expanded in Figures 3.3, 3.4, and 3.5.

Figure 3.2 is expanded in Figures 3.3, 3.4, and 3.5. Though some of the bands are faint and many are clustered in overlapping groups, each band can be seen to be a distinct entity. In fact, some bands can be seen which are not numbered.

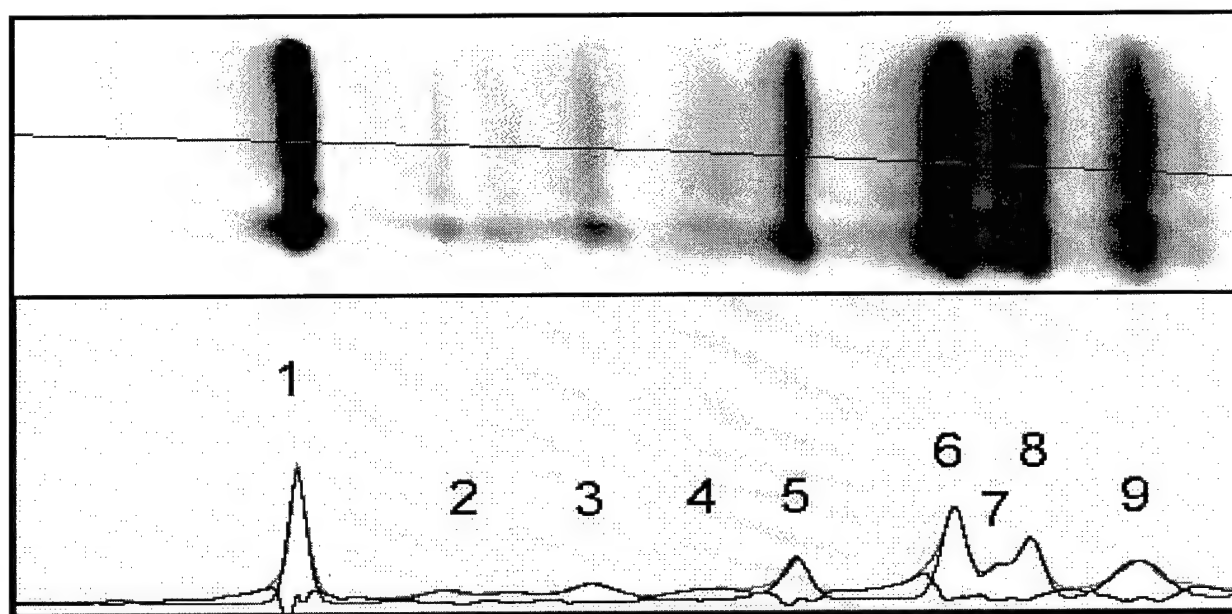


Figure 3.3. Biotinylated proteins 1 through 9. This expands section B of Figure 3.2

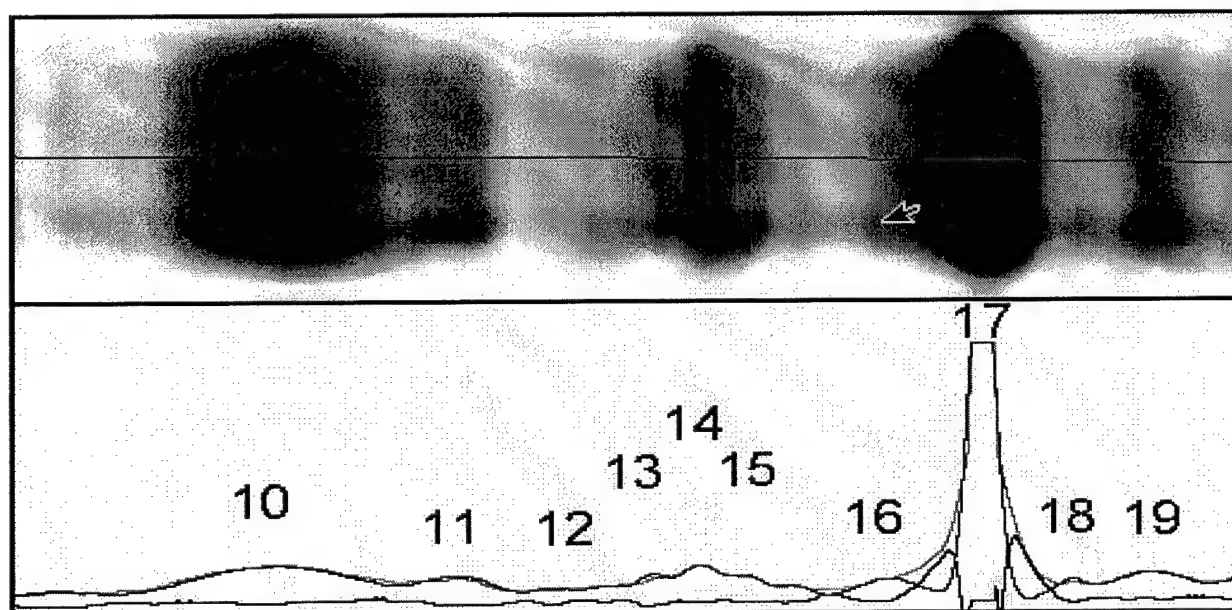


Figure 3.4. Biotinylated proteins 10 through 19. This expands section C of Figure 3.2.

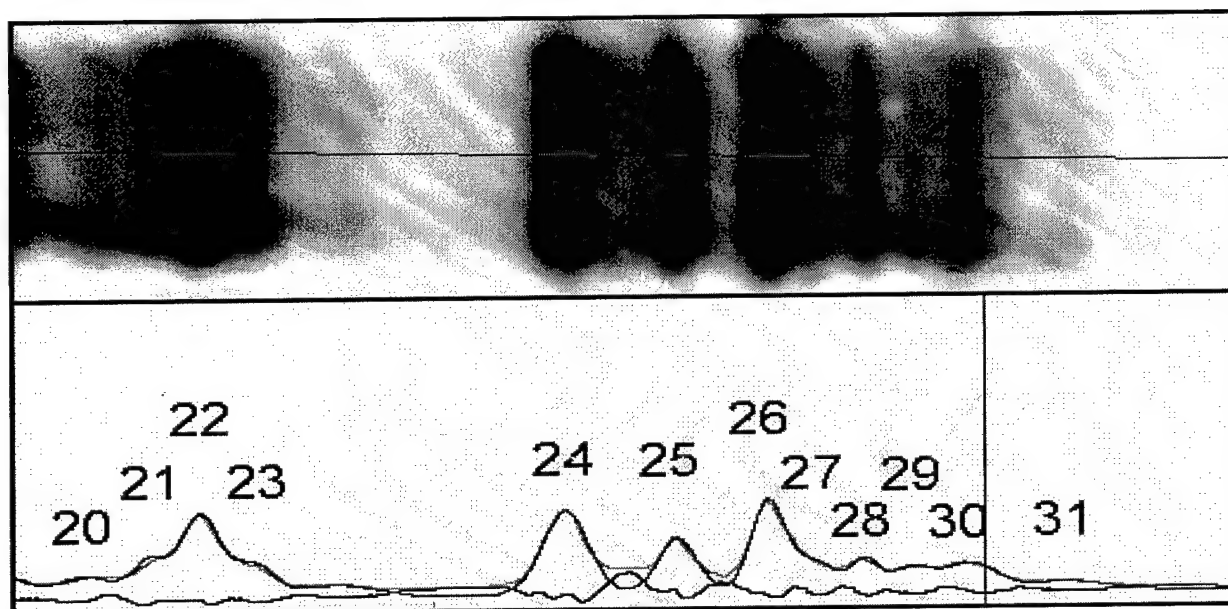


Figure 3.5. Biotinylated proteins 20 through 31. This expands section D of Figure 3.2

AChE and BChE in the mouse brain extract. The amount of AChE and BChE protein in the mouse brain extract was calculated from measurements of AChE and BChE activity. The 0.1 units/ml of AChE activity represents 2×10^{-10} moles/Liter of AChE protein; this was calculated from a specific activity of 6300 units/mg and a molecular weight of 70,000. The 0.006 units/ml of BChE activity represents 1×10^{-10} moles/Liter of BChE protein; this was calculated from a specific activity of 720 units/mg and a molecular weight of 85,000.

It was of interest to know whether there was enough AChE and BChE in the mouse brain extract to see biotinylated AChE and biotinylated BChE on the gel. A loading of 24 μ l per lane means that 5 fmoles of AChE and 2.5 fmoles of BChE were on the gel. The limit of detection is estimated to be in the range of 10-100 fmoles. Thus,

the endogenous AChE and BChE in mouse brain extract is probably too low to be one of the 29 bands seen in Figure 3.1.

Discussion

A method for labeling a protein extract with FP-biotin, of separating the labeled proteins by polyacrylamide gel electrophoresis, and of visualizing the biotinylated proteins has been developed. The best method for visualizing the biotinylated proteins was to hybridize a blot with StreptAvidin conjugated to a fluorophore and measure the fluorescence intensity in an Infrared Imaging System. This system gave reproducible results, good resolution, and better quantitation of band intensities than a method that

measured chemoluminescence of horse radish peroxidase on x-ray film.

It was possible to reproducibly separate and quantitate 32 biotinylated protein bands. The biotinylated proteins ranged in size from 10 to 100 kDa. Three bands were endogenous biotinylated proteins, but the other 29 bands were products of the reaction with FP-biotin. Reaction times up to 7 hours were required to achieve maximum labeling.

Preliminary identification of a few of the FP-biotin labeled proteins can be made by comparing our results to the literature. Eight FP-biotin reactive proteins from rat testis supernatant have been identified by Kidd et al.

[2001]. Three, with molecular weights around 80 kDa, would be expected to travel in the vicinity of bands 5 to 9. They are acyl peptide hydrolase (82 kDa), prolyl oligopeptidase (80 kDa) and carboxylesterase 1 (80 kDa). Carboxylesterase 10 (60 kDa) would migrate at the position of band 10. Long Chain acyl CoA hydrolase (48 kDa) and LDL-associated PLA2 (45 kDa) would appear in the region of bands 12 to 15. The remaining two, PAF acetylhydrolase α 1 and α 2 would run with bands 20 to 21.

This methodology has enabled us to begin screening for proteins that react with insecticide OP.

Task 5

The reactivity with insecticides of the new biochemical markers will be compared to the reactivity of AChE and BChE with the same insecticides. The set of proteins identified in task 3, as well as AChE and BChE, will be ranked for reactivity with chlorpyrifos oxon, dichlorvos, diazinon-O-analog, and malathion-O-analog. This will be accomplished by measuring second order rate constants for individual proteins in brain extracts.

Work on task 5 has begun with chlorpyrifos oxon.

Abstract. Rate constants were estimated for the reaction of FP-biotin with proteins from mouse brain. Second order rate constants ranged from 1×10^3 to $5 \times 10^4 \text{ M}^{-1} \text{ min}^{-1}$ for 13 proteins. First order rate constants ranged from 0.015 to 0.25 min^{-1} for 11 proteins. A method was developed for screening the reactivity of chlorpyrifos oxon with all the proteins in an extract of mouse brain, on one gel.

Introduction. Our goal is to identify proteins that react with OP insecticides at doses that do not have a significant effect on AChE activity. We believe that proteins more reactive than AChE exist, because mice that have no AChE are more sensitive than wild-type mice to the toxicity of OP. Furthermore, low dose exposure may account for chronic symptoms seen in some of our Gulf War veterans. In this section we have applied the methods developed in tasks 1 and 3, to begin to measure the reactivity of brain proteins with insecticide OP. In addition new methods were developed to allow measurement of the inhibition potency of chlorpyrifos oxon for a mixture of

proteins in a brain extract.

Methods

Preparation of mouse brain extracts, separation on SDS-PAGE, transfer of proteins to PVDF membrane, hybridization with StreptAvidin conjugated to a fluorophore, and visualization of the fluorescent label with an Infrared Image Analyzer are described in Task 3.

Kinetics for the reaction of FP-biotin with mouse brain supernatant. Mouse brain supernatant (100,000xg) was reacted with 2-40 μM FP-biotin. Typically, seventeen separate 100 μl reaction mixtures were prepared. Each contained 1.25 mg protein/ml and a constant concentration of FP-biotin, in 50 mM Tris/Cl buffer, pH 8.0, containing 5 mM EDTA and 2.4% methanol. Each reaction mixture was incubated for a defined time (between 0 and 450 minutes); and stopped by adding 20 μl of 0.2 M Tris/Cl buffer, pH 6.8 containing 10% SDS, 30% glycerol, 0.6 M dithiothreitol, and 0.012% bromophenol blue; followed by heating at 80°C for 5 minutes. Aliquots of each reaction were then subjected to SDS-PAGE electrophoresis, and Western blotting with StreptAvidin-Alexa 680 to label the biotinylated proteins; the fluorescence signals were collected, and the signal intensity quantitated.

Results

Rate constants for reaction with FP-biotin. In the course of various experiments, as many as 62 biotinylated-protein bands were

identified. Many of those were very weak and were not reproducible. Some of the bands were shoulders on major bands and probably represented non-Gaussian tailing. Three bands were from endogenous, biotinylated proteins (bands 1, 7, and 8). About 35 protein bands appeared to be from distinct proteins, and gave data over a wide enough range of time points (for

at least one concentration of FP-biotin) that apparent first-order rate constant calculations could be attempted. Rate constants were generally calculated by fitting the {fluorescence intensity} versus {incubation time} data to a single exponential expression. See Figure 5.1 for examples of the rate traces.

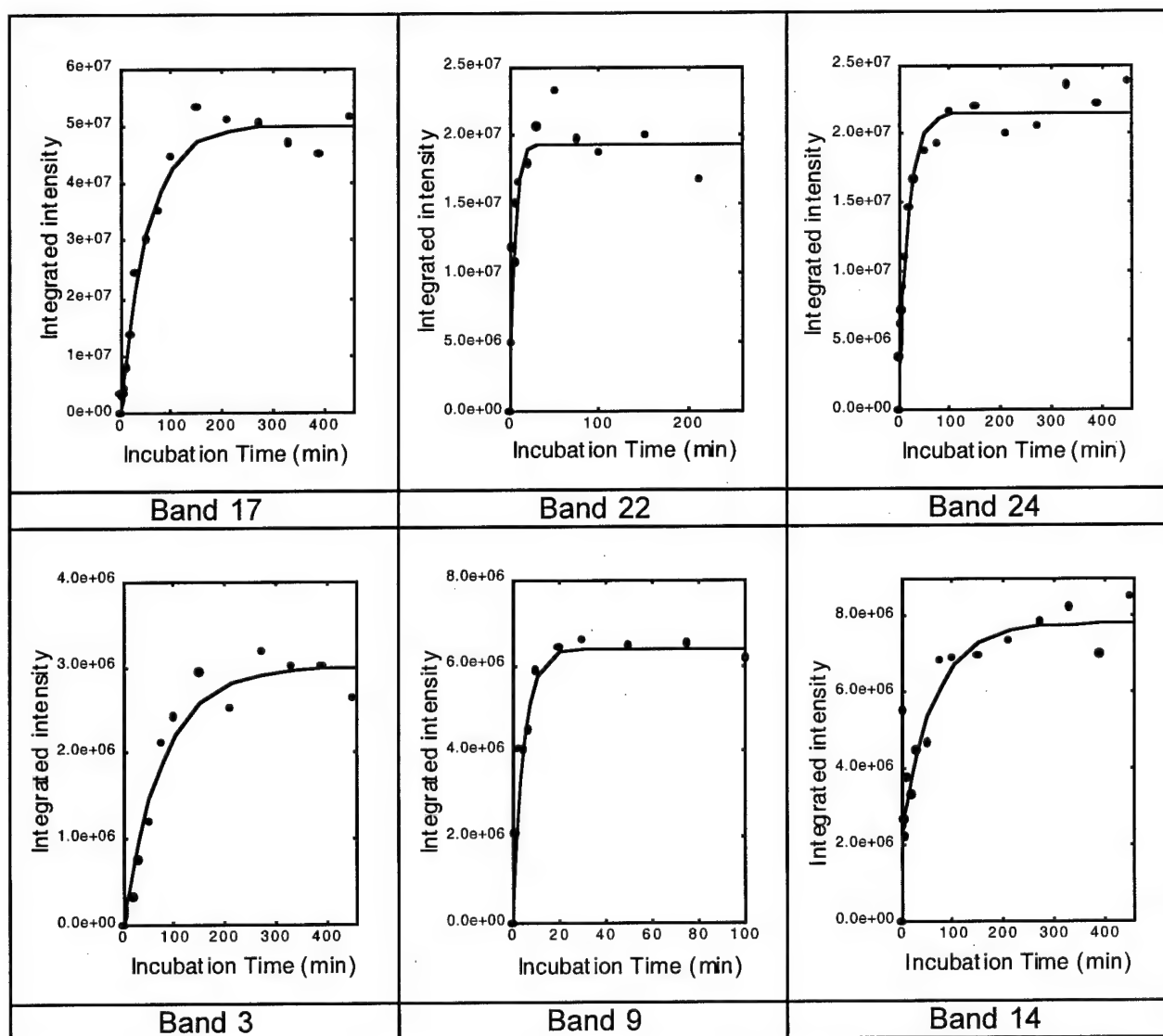


Figure 5.1. Examples of the reaction time course for the reaction of 10 μ M FP-biotin with selected proteins from mouse brain supernatant. The points are the measured data and the line is a fit to a single exponential expression.

Five proteins gave biphasic reactions, especially at 40 μM FP-biotin (see Table 5.1). In those cases, rate constants were calculated by fitting the {fluorescence intensity} versus {incubation time} data to a double exponential expression. Of the 35 proteins for which first-order rate constant calculations were attempted, apparent first-order rate constants were obtained for 29 (at two or more concentrations of FP-biotin). The apparent first-order rate constants typically carried standard deviations of $\pm 30\%$, though some were accurate to $\pm 10\%$ while others were only good to $\pm 50\%$. Reactions for most concentrations of FP-biotin were performed only once, though reactions at 40 μM FPB were repeated.

Reproducibility of the 40 μM data from experiment to experiment varied greatly between bands, i.e. being about $\pm 20\%$ for band 11 or band 8a, and about $\pm 50\%$ for band 14 or 16. In view of the errors involved in data collection, the rate constants listed in Table 5.1 must be considered approximate.

Plotting {apparent first-order rate constant} versus {FP-biotin concentration} revealed that thirteen proteins (45%) reacted in a second-order fashion with FP-biotin; this means the reactions were beginning to saturate and second-order kinetics could be estimated from the points at low FP-biotin concentration. See Figure 5.2 for examples of the second-order plots and Table 5.1 for a list of the rate constants.

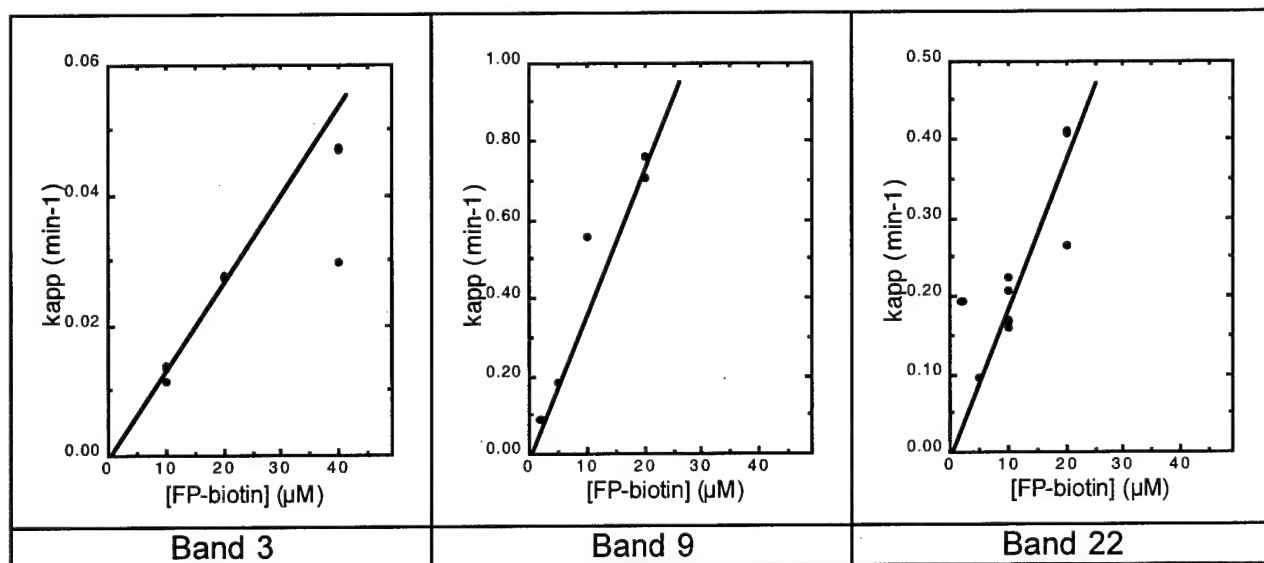


Figure 5.2. Examples of second-order kinetics for the reaction of FP-biotin with selected proteins from mouse brain supernatant. The points are the measured data, and the lines are drawn to give the best fit.

Eleven proteins (38%) showed zero-order dependence on FP-biotin concentration, suggesting that non-covalent binding of FP-biotin by these proteins was saturating at all concentrations of FP-biotin used. See Figure 5.3 for examples of the zero-order plots and Table 5.1 for a list of the rate constants. The apparent rate constants for five proteins (18%) showed either decreasing dependence on FP-biotin

concentration or erratic dependence. See Figure 5.4 for examples of the plots.

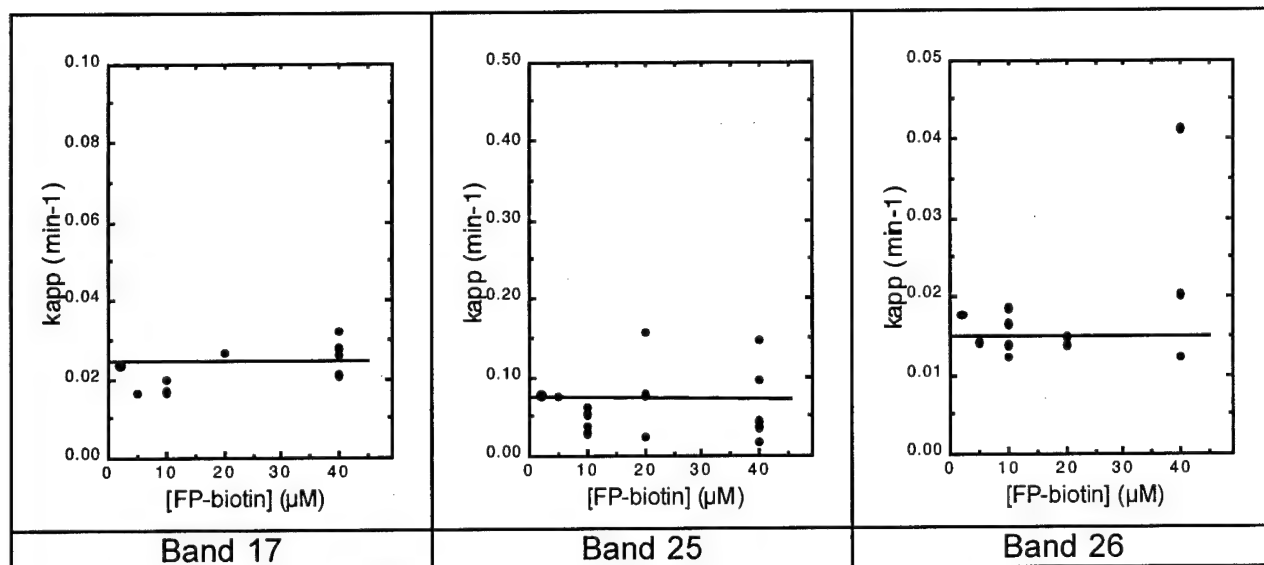


Figure 5.3. Examples of zero-order kinetics for the reaction of FP-biotin with selected proteins from mouse brain supernatant. The points are the measured data, and the lines are drawn to best fit the data.

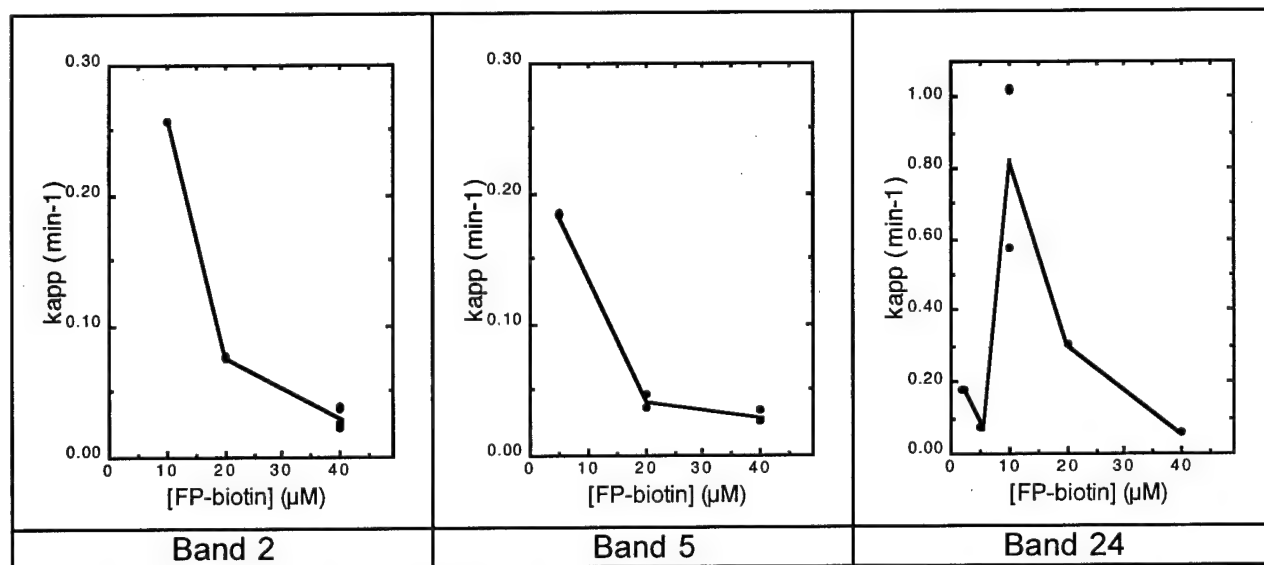


Figure 5.4. Examples of decreasing and erratic dependence of k_{app} on FP-biotin concentration, with selected proteins from mouse brain supernatant. The points are the measured data, and the lines are drawn to illustrate the trends in the data.

All of the proteins (bands), for which rate constants are listed (Table 5.1), were distinctly visible on the Western blot (see Figures 3.3, 3.4, 3.5). They were not shoulders or non-Gaussian artifacts. Many of the bands were in overlapping clusters,

which made deconvolution somewhat subjective and contributed to the uncertainty in the analysis.

Table 5.1. Rate constants for the reaction of FP-biotin with proteins in mouse brain.

Band #	2 ^o rate M ⁻¹ min ⁻¹	1 ^o rate (zero order reactions) min ⁻¹	biphasic
1	endogenous biotinylated protein		
2	decreasing	-	no
3	1.4x10 ³	-	no
4	1.2x10 ³	-	no
5	decreasing	-	no
6	2.5x10 ⁴	-	at 40 µM
7	endogenous biotinylated protein		
8	endogenous biotinylated protein		
9	3.7x10 ⁴	-	10 to 40 µM
10	-	0.019	no
11	2.2x10 ³	-	no
12	1.8x10 ³	-	no
13	-	0.026	no
14	-	0.016	no
15	1.1x10 ³	-	no
16	-	0.020	no
17	-	0.026	no
18	1.8x10 ³	-	no
19	2.0x10 ³	-	no
20	-	0.16	no
21	decreasing	-	no
22	1.7x10 ⁴	-	at 40 µM
23	-	0.25	no
24	erratic	-	10 to 40 µM
25	-	0.072	at 40 µM
26	-	0.015	no
27	6.5x10 ³	-	at 20 M
28	1.4x10 ⁴	-	no
29	5.3x10 ⁴	no	17
30	-	0.09	at 10 & 40 µM
31	decreasing	-	no
32	-	0.14	no

Reaction of chlorpyrifos-oxon with mouse brain supernatant.

Original proposal. It was originally proposed that the kinetics for the reaction of four insecticides with proteins in mouse brain sub-cellular fractions be studied (chlorpyrifos-oxon, diazinon-O-analog, dichlorvos, and malathion-O-analog). Kinetics were to be determined by incubating the brain fraction with a fixed concentration of the insecticide for varying times; stopping the reaction by gel filtration over a spin column; and then reacting the filtrate with FP-biotin to label the remaining organophosphate-reactive proteins. Disappearance of biotinylatable protein would provide a measure for the extent of the reaction with the insecticide, allowing calculation of a first-order rate constant for the insecticide at the concentration used. Repeating this reaction scheme at different concentrations of insecticide would generate a set of first-order rate constants, from which a second-order rate constant could be calculated and compared to the second-order rate constant for the reaction of that insecticide with AChE or BChE. The process was patterned after a study by Richards et al. [1999], using tritiated diisopropylfluorophosphate to follow the reaction progress. Though reasonable, this procedure would be laborious; a separate SDS-PAGE would have to be processed for each first-order rate constant. Therefore, we chose to try determining the second-order rate constant for the insecticide by direct competition with FP-biotin in a single reaction.

Competitive reaction scheme. The competition method is predicated upon the fact that when a compound is

mixed with two irreversible reactants; and the reaction is allowed to run to completion; the ratio of the products is equal to the ratio of the apparent first-order rate constants [see Frost and Pearson for a derivation of the equations]. If the rate constant for one of the reactants is known, and the product from that reaction can be monitored, then the rate constant for the other reactant can be determined from the effect that its presence has on product formation by the first reactant. Pairing FP-biotin with other organophosphates for reaction with organophosphate-reactive proteins was a good fit to this type of analysis. First, organophosphates are irreversible reactants. Next, the second-order rate constants for FP-biotin reacting with 13 proteins from the mouse brain supernatant had already been determined (Table 5.1). Finally, product formation from reactions with FP-biotin were readily measured. If aliquots of mouse brain supernatant were mixed with a fixed concentration of FP-biotin and varying concentrations of insecticide, and if the reactions were allowed to reach completion, then the apparent first-order rate constant for the reaction of each protein with each concentration of the insecticide could be calculated from the measured amount of FP-biotin-modified protein remaining at the end of the reaction. From those apparent first-order rate constants, the second-order rate constants could be calculated. A complete data set could be collected from a single SDS-PAGE. Even the proteins showing zero-order kinetics with FP-biotin could be evaluated; they could be given a lower limit value for a second-order rate constant. This concept was quite appealing in theory,

but proved to be deceptively unproductive in practice.

The competitive scheme was attempted with chlorpyrifos-oxon. Mouse brain supernatant (1.25 mg protein/ml) was reacted with 5 μ M FP-biotin and 0.05-19.2 μ M chlorpyrifos-oxon for 450 minutes at 25°C in 50 mM Tris/Cl buffer, pH 8.0, containing 5 mM EDTA and 2.4% methanol. Reactions were stopped by adding 1/5 volume of 0.2 M Tris/Cl buffer, pH 6.8, containing 10% SDS, 30% glycerol, 0.6 M dithiothreitol and 0.012% bromophenol blue and heating to 85°C for 5 minutes. Aliquots from each reaction mixture were separated on 10-20% SDS-PAGE, transferred to PVDF membrane, reacted with Streptavidin-Alexa 680, the fluorescence signals from the biotinylated proteins were collected with Odyssey, and quantitated using Kodak 1D software. To a first approximation, the procedure worked as expected, i.e. the biotin signal intensities decreased as the chlorpyrifos-oxon concentration increased. However, the noise in the signal measurement, which was tolerable for determination of the FP-biotin kinetics (see Figure 5.1), became excessive for purposes of this competitive scheme. This was because determination of the apparent first-order rate constant required taking a ratio of the FP-biotin signal in the absence of chlorpyrifos-oxon to that in the presence of chlorpyrifos-oxon. That ratio amplified the noise to a point where only the most prominent signal changes were reliable.

Data were collected on 9 of the 29 organophosphate-reactive proteins. Second-order rate constants for the reaction with chlorpyrifos oxon were obtained for 4 proteins (band 6: 5×10^3

$\text{M}^{-1}\text{min}^{-1}$; band 9: $5 \times 10^3 \text{ M}^{-1}\text{min}^{-1}$; band 19: $7 \times 10^2 \text{ M}^{-1}\text{min}^{-1}$; and band 22: $2 \times 10^4 \text{ M}^{-1}\text{min}^{-1}$). Lower limits for the second-order rate constants were obtained for 2 proteins (band 23: $1 \times 10^6 \text{ M}^{-1}\text{min}^{-1}$; and band 25: $7 \times 10^4 \text{ M}^{-1}\text{min}^{-1}$).

Rate constants could not be calculated for 3 of the chlorpyrifos-oxon reactive proteins because the reactions of those proteins with FP-biotin gave decreasing or erratic dependence on FP-biotin concentration (bands 5, 21, and 24). Of these nine proteins, band 23 is the most interesting, in that it reacts with chlorpyrifos-oxon at a rate close to that of AChE (mouse: $5 \times 10^6 \text{ M}^{-1}\text{min}^{-1}$; human: $4 \times 10^6 \text{ M}^{-1}\text{min}^{-1}$ from Amitai et al., 1998).

IC50 scheme. In view of these limitations, it was decided to use a different scheme for determination of the relative reactivity of mouse brain proteins toward insecticides. Yet, it was still desirable to collect a complete data set on a single SDS-PAGE. To accomplish this, an IC50 approach is currently being explored. IC50 stands for the concentration of inhibitor necessary to obtain 50% inhibition. An IC50 is easy to determine; and it is not dependent upon the mechanism by which the inhibitor reacts with the target. It requires only that some means of determining the fraction of inhibition exist. For that purpose, the FP-biotin reaction will suffice. The general scheme for determining the IC50 in this case consists of reacting aliquots of a mouse brain fraction with varying amounts of insecticide, for a fixed time; stopping the reaction; reacting the remaining organophosphate-reactive proteins with FP-biotin; and then determining the amount of biotinylated protein. The whole series of reactions can be made

at one time, and the results determined on a single SDS-PAGE. The amount of insecticide which results in 50% loss of the FP-biotin signal is the IC₅₀. By adding AChE to the reaction mixture, a direct comparison of IC₅₀ for the unknown proteins to IC₅₀ for AChE can be made.

Most of the steps in this IC₅₀ scheme have already been discussed. Only the means for stopping the reaction is new. The stopping step must leave the proteins undenatured so that they can react with FP-biotin in the following step. To accomplish this, it was decided to separate the insecticide from the proteins by gel filtration using a spin column.

Test of the spin columns. We tested a series of columns: the MicroSpin G-25 (Amersham), which uses Sephadex G-25; the Performa SR (Edge Biosystems), which uses a proprietary matrix; a homemade Sephadex G-25 (fine) column on an Ultrafree-MC 0.22 µm support (Millipore); a homemade Sephadex G-25 (fine) column on an Ultrafree-MC/HV 0.45 µm support (Millipore); a homemade Sephadex G-25 (fine) column on a Performa SR support; and a homemade Sephadex G-10 column on a Performa SR support. All columns were 0.6-0.8 ml in volume. They were tested first for retention of lysozyme. Lysozyme was used because its small molecular weight makes it representative of proteins most likely to be retained on the matrix. Next, they were tested for retention of chlorpyrifos-oxon. A mixture of lysozyme and chlorpyrifos-oxon was passed through the column, and the effluent was assayed for capacity to inhibit BChE turnover. Finally, they were tested for re-usability after the

matrix was washed.

Tests were made as follows: The column was equilibrated with 50 mM Tris/Cl buffer, pH 8.0, containing 5 mM EDTA by suspending the resin in the buffer, while the resin was still in the column, and then centrifuging it at 740xg for 3 minutes in a Sorval MC 12V microcentrifuge, to remove excess buffer. This was repeated three times. One hundred microliters of the test sample (1 mg/ml lysozyme or 1 mg/ml lysozyme plus 10 µM chlorpyrifos-oxon) was applied to the equilibrated/centrifuged column, and then it was centrifuged for 1 minute at 740xg. The absorbance of the effluent at 280 nm was compared to the 280 nm absorbance of the starting lysozyme, to assess retention of lysozyme. Ten microliters of the effluent was added to a reaction of BChE with 1 mM butyrylthiocholine (in 0.1 M potassium phosphate buffer, pH7.0), and the apparent rate for inhibition of the reaction was compared to a chlorpyrifos-oxon standard curve. It was found that all 100 µl of the test sample passed through each column. At least 70% of the lysozyme passed through all columns. The discriminating factor was retention of chlorpyrifos-oxon. The homemade columns allowed about 3% of the chlorpyrifos-oxon to pass; the MicroSpin G-25 passed 1-1.5%; while the Performa SR allowed only 0.5% of the chlorpyrifos-oxon to pass. The Performa SR column reduced the concentration of chlorpyrifos-oxon by 200-fold, which should suffice to effectively stop the reaction. Support for stopping the chlorpyrifos-oxon reaction will come from the addition of the FP-biotin, which will compete with any residual chlorpyrifos-oxon. The same

level of separation-performance was obtained when the columns were re-equilibrated with buffer and re-used.

Test of the IC50 scheme.

Aliquots of mouse brain supernatant (1.3 mg protein/ml) were incubated with chlorpyrifos-oxon (0.025 to 19.2 μM) in 50 mM Tris/Cl, buffer, pH 8.0, containing 5 mM EDTA and 2.4% methanol (94 μl total volume) for 30 minutes, at 25°C. Reactions were stopped by gel filtration through a Performa SR spin columns, equilibrated in the same buffer. Then 6 μl of 170 μM FP-biotin were added to each reaction mixture, to yield 10 μM FP-biotin. Incubation was continued for 300 minutes at 25°C. Then the reactions were stopped by adding 20 μl of 0.2 M Tris/Cl, buffer, pH 6.8, containing 10% SDS, 30% glycerol, 0.6

M dithiothreitol and 0.012% bromophenol blue, and heating to 85°C for 5 minutes. Aliquots from each reaction mixture were separated on 10-20% SDS-PAGE, transferred to PVDF membrane, and reacted with Streptavidin-Alexa 680; the fluorescence signals from the biotinylated proteins were collected with Odyssey, and quantitated using Kodak 1D software. Technical difficulties in the Western blotting prevented evaluation of signals from bands 1-9. However, for 11 of the remaining 23 proteins, the biotin levels decreased as the chlorpyrifos-oxon levels increased (see Figure 5.5 for examples of the traces and Table 5.2 for the IC50 values).

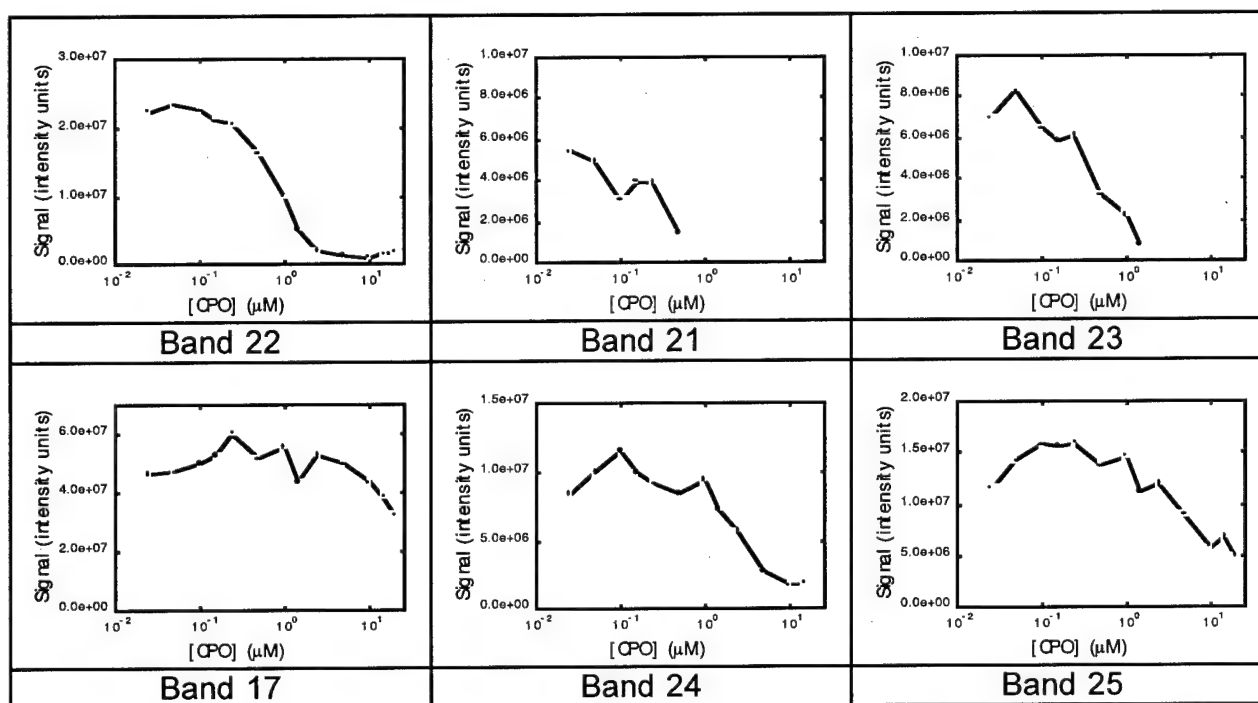


Figure 5.5. Examples of IC50 traces for the reaction of chlorpyrifos oxon with proteins in mouse brain supernatant.

The IC₅₀ values indicated that band 23 was very reactive toward chlorpyrifos-oxon (IC₅₀=0.4 μ M), just as the competitive assay had. But, in addition, bands 20, and 21 (which were not measurable in the competitive assay) showed reactivity comparable to band 23 in the IC₅₀ assay (IC₅₀=0.3 μ M for band 21; IC₅₀=0.2 μ M for band 22). Band 22, the only other band which can be compared between the

two assays, was less reactive than band 23 in both the IC₅₀ and competitive schemes. The results from the IC₅₀ scheme are therefore comparable to those from the competitive scheme, but the IC₅₀ scheme is more robust, being able to return information on more of the proteins from mouse brain supernatant.

Table 5.2. IC₅₀ for the reaction of chlorpyrifos oxon with proteins in mouse brain.

Band #	IC ₅₀ , μ M
10	>20
11	>>20
12	no observable reaction
13	no observable reaction
14	no observable reaction
15	no observable reaction
16	no observable reaction
17	>20
20	0.2
21	0.3
22	0.9
23	0.4
24	3
25	6
26	>>20
28	no observable reaction
30	>>20
31	no observable reaction
32	no observable reaction

The only task remaining in order to complete the IC₅₀ assay, is to incorporate an internal AChE standard into the reaction mixture. This will provide a reference IC₅₀ value for comparison with the IC₅₀ values from the unknown proteins, all obtained under identical conditions.

Discussion

The second-order rate constants for reaction of FP-biotin with proteins of mouse brain supernatant (0.11 - 5.3×10^4 $M^{-1}min^{-1}$, Table 5.1), are all at least 100-fold slower than the rate constant for the reaction of FP-biotin with AChE (3×10^6 $M^{-1}min^{-1}$). The other reactions listed in

Table 5.1, being limited by first-order steps, appear to be even slower. Therefore, *is it reasonable to expect any of these mouse brain proteins to react with other organophosphates at rates faster than AChE?* The simple answer is yes. This is because specificity of AChE for organophosphates would be expected to be different from that of other organophosphate-reactive proteins. Therefore, the pattern of reactivity, which is found for FP-biotin in mouse brain supernatant, does not necessarily represent the pattern of reactivity, which will be found for other organophosphates. This is illustrated by acyl peptide hydrolase.

Acyl peptide hydrolase has been identified as an FP-biotin reactive protein in rat testis supernatant [Liu et al., 1999; Kidd et al., 2001]. It is an 82 kDa protein. It would migrate in the vicinity of bands 5-9 (see Figure 3.1). This protein is also found in rat brain and in porcine brain [Richards et al., 2000] and would be expected to be in mouse brain. Therefore, acyl peptide hydrolase should be one of the cluster of proteins around positions 5-9, in our work. None of these proteins displays abnormally rapid reactivity with FP-biotin, strongly suggesting that acyl peptide hydrolase is not especially reactive with FP-biotin. Therefore, acyl peptide hydrolase should react with FP-biotin more slowly than AChE. On the other hand, acyl peptide hydrolase reacts with other organophosphates more rapidly than AChE. The IC₅₀ values for acyl peptide hydrolase are lower than those for AChE by 6.0-fold (chlorpyrifosmethyl-oxon), 6.6-fold (dichlorvos), 10.6-fold (diisopropylfluorophosphate), and 22-fold (mipafox) [Richards et al., 2000]. Thus, when comparing acyl peptide hydrolase and AChE, relative reactivity with FP-biotin does not define relative reactivity with all

organophosphates.

Conclusions

The purpose of this work is to survey brain tissue for proteins which will react with organophosphate insecticides at doses lower than those to which acetylcholinesterase is sensitive. This year, the groundwork for that survey has been completed.

FP-biotin, the critical tool for detecting organophosphate-reactive proteins in sub-cellular brain fractions has been prepared, purified and tested. It was found to be stable to handling, yet reactive with at least 29 proteins in mouse brain supernatant.

The reactivity of FP-biotin with AChE and BChE was determined. AChE reacted in a simple, second-order fashion with a rate constant of $3.0 \times 10^6 \pm 3.9 \times 10^4 \text{ M}^{-1} \text{ min}^{-1}$. BChE also reacted with FP-biotin in a second-order fashion. The rate constant was $2.8 \times 10^7 \pm 3.0 \times 10^5 \text{ M}^{-1} \text{ min}^{-1}$, if the concentration of FP-biotin was determined by weight. However, BChE appeared to react with a minor component of the FP-biotin preparation (10%), probably a stereoisomeric form of the phosphate. If this factor is taken into consideration, the rate constant will be 10-times faster.

The survey protocol was refined. An IC₅₀ approach for reacting the mouse brain supernatant with insecticides was adopted and reaction conditions defined. The SDS-PAGE and Western blotting protocols were optimized. An improved method for visualizing the biotinylated proteins on the PVDF membrane was adopted and a reliable method for quantitation of the signals was found. The entire procedure was tested with chlorpyrifos-oxon and mouse brain supernatant, and a highly reactive protein (Band 23) was tentatively identified.

Key Research Accomplishments

- A method for screening a mixture of proteins for reactivity with insecticide OP has been developed. The key to the screening method is the use of a biotinylated-OP.
- A method for keeping AChE knockout mice alive to adulthood has been established.
- AChE knockout mice are more sensitive to the lethality of all OP tested to date, including DFP, chlorpyrifos oxon, iso-OMPA, and the nerve agent VX.
- AChE knockout mice have drastically reduced levels of functional muscarinic acetylcholine receptors. They have adapted to the presence of excess acetylcholine by downregulating their receptors for acetylcholine.
- The supersensitivity of AChE knockout mice to OP is explained in part by inhibition of BChE.

Reportable Outcomes

Published manuscript

Duysen EG, Stribley JA, Fry DL, Hinrichs S, Lockridge O. Rescue of the acetylcholinesterase knockout mouse by feeding a liquid diet; phenotype of the adult acetylcholinesterase deficient mouse. *Brain Res Dev Brain Res* 137: 43-54 (2002)

Submitted manuscript

Duysen EG, Li B, Lockridge O. Why is the acetylcholinesterase knockout mouse supersensitive to organophosphorus agent (OP) toxicity? *Proceedings BioScience 2002 Medical Defense Review* (2002)

Abstract

Duysen EG, Stribley JA, Fry DL, Hinrichs S, Lockridge O. Rescue of the acetylcholinesterase knockout mouse by feeding a liquid diet; phenotype of the adult acetylcholinesterase deficient mouse. XI International symposium on Cholinergic Mechanisms-Function and Dysfunction and 2nd Misrahi Symposium on Neurobiology, St. Moritz, Switzerland, May 5-9, 2002.

AChE knockout mice

A colony of AChE knockout mice that lives to adulthood has been established.

Conclusions. Summary of results to include the implications of the research.

The methods developed in this first year of the grant provide the groundwork for achieving the goals of this research. Our goal is to identify new biological markers of OP exposure.

References.

- Amitai G, Moorad, D, Adani R, Doctor BP. Inhibition of acetylcholinesterase and butyrylcholinesterase by chlorpyrifos-oxon, *Biochem Pharmacol* 56: 293-299 (1998).
- Bomser JA, Casida JE. Diethylphosphorylation of rat cardiac M2 muscarinic receptor by chlorpyrifos oxon in vitro. *Toxicol Lett* 119: 21-26 (2001).
- Donger C, Krejci E, Serradell AP, Eymard B, Bon S, Nicole S, Chateau D, Gary F, Fardeau M, Massoulié J, Guicheney P. Mutation in the human acetylcholinesterase-associated collagen gene, COLQ, is responsible for congenital myasthenic syndrome with end-plate acetylcholinesterase deficiency (Type Ic). *Am J Hum Genet* 63: 967-975 (1998).
- Doorn JA, Schall M, Gage DA, Talley TT, Thompson CM, Richardson RJ. Identification of butyrylcholinesterase adducts after inhibition with isomalathion using mass spectrometry: difference in mechanism between (1R)- and (1S)- stereoisomers. *Toxicol Appl Pharmacol* 176: 73-80 (2001)
- Duysen EG, Li B, Xie W, Schopfer LM, Anderson RS, Broomfield CA, Lockridge O. Evidence for non-acetylcholinesterase targets of organophosphorus nerve agent; supersensitivity of the acetylcholinesterase knockout mouse to VX lethality. *J. Pharmacol. Exp. Ther.* 299: 542-550 (2001).
- Duysen EG, Li B, Lockridge O. Why is the acetylcholinesterase knockout mouse supersensitive to organophosphorus agent (OP) toxicity? *Proceedings BioScience 2002 Medical Defense Review* (2002a)
- Duysen EG, Stribley JA, Fry DL, Hinrichs S, Lockridge O. Rescue of the acetylcholinesterase knockout mouse by feeding a liquid diet; phenotype of the adult acetylcholinesterase deficient mouse. *Brain Res Dev Brain Res* 137: 43-54 (2002b)
- Ellman GL, Courtney KD, Andres V Jr, Featherstone RM. A new and rapid colorimetric determination of acetylcholinesterase activity. *Biochem Pharmacol* 7: 88-95 (1961)
- Feng G, Krejci E, Molgo J, Cunningham JM, Massoulié, Sanes JR. Genetic analysis of collagen Q: roles in acetylcholinesterase and butyrylcholinesterase assembly and in synaptic structure and function. *J Cell Biol* 144: 1349-1360 (1999).
- Frost AA, Pearson RG in Kinetics and Mechanism 2nd edition pp160-162 (1961); John Wiley & Sons, Inc; New York.
- Gomez J, Shannon H, Kostenis E, Felder C, Zhang L, Brodtkin J, Grinberg A, Sheng H, Wess J. Pronounced pharmacologic deficits in M2 muscarinic acetylcholine receptor knockout mice. *Proc Natl Acad Sci USA* 96: 1692-1697 (1999).
- Gray EG, Whittaker VP. The isolation of nerve endings from brain: An electron-microscopic study of cell fragments derived by homogenization and centrifugation, *J Anat* 96: 79-88 (1962).
- Green NM. A spectrophotometric assay for avidin and biotin based on binding of dyes by avidin, *Biochem J* 94: 23c-24c (1965).
- Huff RA, Corcoran JJ, Anderson JK, Abou-Donia MB. Chlorpyrifos oxon binds directly to muscarinic receptors and inhibits cAMP accumulation in rat striatum. *J Pharmacol Exp Ther* 269: 329-335 (1994).

- Kidd D, Liu Y, Cravatt BF. Profiling serine hydrolase activities in complex proteomes, *Biochemistry* 40: 4005-4015 (2001).
- Laemmli UK. Cleavage of structural proteins during the assembly of the head of bacteriophage T4, *Nature* 227: 680-685 (1970).
- Li B, Stribley JA, Ticu A, Xie W, Schopfer LM, Hammond P, Brimijoin S, Hinrichs SH, Lockridge O. Abundant tissue butyrylcholinesterase and its possible function in the acetylcholinesterase knockout mouse, *J. Neurochem.* 75: 1320-1331 (2000).
- Liu Y, Patricelli MP, Cravatt BF. Activity-based protein profiling: The serine hydrolases, *Proc Natl Acad Sci USA* 96: 14694-14699 (1999).
- McDonough JH, Shih TM. Neuropharmacological mechanisms of nerve agent-induced seizure and neuropathology. *Neurosci Biobehav Rev* 21: 559-579 (1997).
- Mesulam MM, Guillozet A, Shaw P, Levey A, Duysen EG, Lockridge O. Acetylcholinesterase knockouts establish central cholinergic pathways and can use butyrylcholinesterase to hydrolyze acetylcholine *Neuroscience* 110: 627-639 (2002).
- Millard CB, Lockridge O, Broomfield CA. Organophosphorus acid anhydride hydrolase activity in human butyrylcholinesterase: synergy results in a somanase. *Biochemistry* 37: 237-247 (1998).
- Moser VC. Comparisons of the acute effects of cholinesterase inhibitors using a neurobehavioral screening battery in rats. *Neurotoxicol Teratol* 17: 617-625 (1995).
- Ohno K, Brengman J, Tsujino A, Engel AG. Human endplate acetylcholinesterase deficiency caused by mutations in the collagen-like tail subunit (ColQ) of the asymmetric enzyme. *Proc Natl Acad Sci USA* 95: 9654-9659 (1998).
- Pope CN. Organophosphorus pesticides: do they all have the same mechanism of toxicity? *J Toxicol Environ Health B Crit Rev* 2: 161-181 (1999).
- Richards PG, Johnson MK, and Ray, DE Identification of acylpeptide hydrolase as a sensitive site for reaction with organophosphorus compounds and a potential target for cognitive enhancing drugs, *Mol Pharmacol* 58: 577-583 (2000).
- Richards P, Johnson M, Ray D, and Walker C Novel protein targets for organophosphorus compounds, *Chem Biol Inter* 119: 503-511 (1999).
- Xie W, Stribley JA, Chatonnet A, Wilder PJ, Rizzino A, McComb RD, Taylor P, Hinrichs SH, Lockridge O. Postnatal developmental delay and supersensitivity to organophosphate in gene-targeted mice lacking acetylcholinesterase, *J. Pharmacol. Exp. Ther.* 293: 896-902 (2000).

Appendices

- 1) Duysen EG, Stribley JA, Fry DL, Hinrichs S, Lockridge O. Rescue of the acetylcholinesterase knockout mouse by feeding a liquid diet; phenotype of the adult acetylcholinesterase deficient mouse. *Brain Res Dev Brain Res* 137: 43-54 (2002)
- 2) **Abstract** Duysen EG, Stribley JA, Fry DL, Hinrichs S, Lockridge O. Rescue of the acetylcholinesterase knockout mouse by feeding a liquid diet; phenotype of the adult acetylcholinesterase deficient mouse. XI International symposium on Cholinergic Mechanisms-Function and Dysfunction and 2nd Misrahi Symposium on Neurobiology, St. Moritz, Switzerland, May 5-9, 2002.

Research report

Rescue of the acetylcholinesterase knockout mouse by feeding a liquid diet; phenotype of the adult acetylcholinesterase deficient mouse

Ellen G. Duysen^a, Judith A. Stribley^{a,b}, Debra L. Fry^a, Steven H. Hinrichs^b,
Oksana Lockridge^{a,*}

^a*Eppley Institute, University of Nebraska Medical Center, Omaha, NE 68198-6805, USA*

^b*Department of Pathology and Microbiology, University of Nebraska Medical Center, Omaha, NE 68198-6495, USA*

Accepted 22 March 2002

Abstract

Acetylcholinesterase (AChE, EC3.1.1.7) functions in nerve impulse transmission, and possibly as a cell adhesion factor during neurite outgrowth. These functions predicted that a mouse with zero AChE activity would be unable to live. It was a surprise to find that AChE $-/-$ mice were born alive and survived an average of 14 days. The emaciated appearance of AChE $-/-$ mice suggested an inability to obtain sufficient nutrition and experiments were undertaken to increase caloric intake. Pregnant and lactating dams (+/-) were fed 11% high fat chow supplemented with liquid Ensure[®]. AChE $-/-$ pups were weaned early, on day 15, and fed liquid Ensure. Although nullizygous animals showed slow but steady weight gain with survival over 1 year (average 100 days), they remained small at all ages compared to littermates. They demonstrated delays in temperature regulation (day 22 vs. 15), eye opening (day 13 vs. 12), righting reflex (day 18 vs. 12), descent of testes (week 7–8 vs. 4), and estrous (week 15–16 vs. 6–7). Significant physical findings in adult AChE $-/-$ mice included body tremors, abnormal gait and posture, absent grip strength, inability to eat solid food, pinpoint pupils, decreased pain response, vocalization, and early death caused by seizures or gastrointestinal tract ileus. Behavioral deficits included urination and defecation in the nest, lack of aggression, reduced pain perception, and sexual dysfunction. These findings support the classical role for AChE in nerve impulse conduction and further suggest that AChE is essential for timely physical development and higher brain function. © 2002 Elsevier Science B.V. All rights reserved.

Theme: Development and regeneration

Topic: Neurotransmitter systems and channels

Keywords: Postnatal development; Gene targeting; Under-nutrition; Acetylcholinesterase depletion

1. Introduction

Acetylcholinesterase has a central role in neurotransmission at cholinergic synapses. AChE hydrolyzes acetylcholine, thus preventing overstimulation of nicotinic and muscarinic receptors. Overstimulation of these receptors may lead to respiratory failure and death. AChE has been proposed to have a second function independent of its catalytic activity [1–4,9,11,13–16,23,25,26,28,30–32], possibly serving as a cell adhesion factor in morphogenesis

of neurites. These important roles for AChE predicted that the absence of AChE activity in mutant mice would be lethal. It was a surprise, therefore, to find that mice with no AChE enzyme activity and no AChE protein were born alive, and that they were capable of breathing and moving [35]. They were not normal, however. Homozygous mutant mice were smaller than heterozygous littermates, they gained body weight more slowly, their eyes never opened, they had no righting reflex, the external ear did not mature, body tremor was persistent, they circled when walking, and they died at an early age. About 50% of the nullizygotes died by postnatal day 14 and 100% died by day 21 ($n=63$). This phenotype could be due to deficiency in cholinergic neurotransmission caused by absence of AChE enzyme activity, or to developmental problems caused by

*Corresponding author. Tel.: +1-402-559-6032; fax: +1-402-559-4651.

E-mail address: olockrid@unmc.edu (O. Lockridge).

the absence of the AChE protein, or to a combination of both.

In the present work our goal was to prolong the life of AChE $-/-$ mice. Injection of purified AChE or of atropine had no beneficial effect, so we tried a different approach. Their emaciated appearance and absence of body fat suggested that the cause of death might be starvation. Therefore, efforts were made to increase their caloric intake. This report describes the success of feeding dams a high fat diet supplemented with liquid Ensure[®] to enrich their milk during the nursing period. After weaning, the AChE $-/-$ mice subsist on liquid Ensure. This diet increased the lifespan of AChE $-/-$ mice to an average of 100 days. Several AChE $-/-$ mice have lived up to 15 months.

Having succeeded in producing an abundant supply of AChE $-/-$ mice, we were able to investigate which characteristics were due to deficiency of AChE catalytic activity. Since pinpoint pupils, body tremor, and muscle weakness are present in AChE $-/-$ mice and are also diagnostic for poisoning by AChE inhibitors, we concluded that these abnormalities were due to lack of AChE catalytic function. However, other abnormalities, including postnatal developmental delay, low body weight, lack of housekeeping behavior, and sexual dysfunction have no obvious link to absence of AChE catalytic function and could be due to a combination of effects.

2. Materials and methods

2.1. Mice

Animal studies were carried out in accordance with the Guide for the Care and Use of Laboratory Animals as adopted by the US National Institutes of Health. AChE knockout mice were produced by homologous recombination [34,35]. Exons 2, 3, 4, and 5 of the ACHE gene were deleted, making it impossible to produce an AChE protein. The colony was maintained by breeding AChE $+/-$ mice. The animals are in a strain 129Sv genetic background, produced by mating the chimera (originating from R1 embryonic stem cells) to strain 129Sv mice (Taconic 129S6/SvEvTac). Mice are housed in a barrier facility at a temperature of 66–74 °F, humidity of 40–42%. Lights are on for 12 h a day.

2.2. Genotyping mice

Mice were genotyped by PCR. The preparation of genomic DNA and the PCR primers were different from those published earlier [35]. Genomic DNA was isolated from the hair roots of mice 14 days of age or older, by the method of Schmitteckert et al. [27]. A tuft of hair roots

was placed in a 0.5-ml microfuge tube. After the addition of 50 μ l of 0.05 M NaOH, the tubes were heated at 95 °C for 5 min in the thermocycler, and then cooled to 4 °C. The DNA concentration, estimated from absorbance at 260 nm, ranged from 0.15 to 1.4 μ g/ μ l depending on the number of hair roots. A 10- μ l PCR reaction was set up to contain a total of 0.35 μ g DNA, 0.25 units of HotStar Taq Polymerase (Qiagen Inc., Valencia, CA), 0.2 mM of each dNTP, 0.02 μ g of each primer, and 1 μ l of PCR Enhance Solution (Gibco-BRL #52391). Primers for wild-type ACHE were 21mer sense (5'AATGACACCGAGCTGATAGCC) and 22mer antisense (5'CCAGTATTGATGAGAGCCTCCG), both located within exon 2 of ACHE. Primers for the ACHE knockout allele were 25mer sense (5'AATGGGCAGGTAGCCGGATCAAGCG) in the NEO gene and 25mer antisense (5'CGTAGTCTCGTCGGCTACAGACAA) also in the NEO gene. The wild-type allele produced a band of 164 bp, whereas the knockout allele had a band of 322 bp. HotStar Taq Polymerase was activated by heating at 95 °C for 15 min. The DNA was denatured at 94 °C for 1 min 15 s, annealed at 60 °C for 1 min 30 s, and extended at 72 °C for 1 min 30 s in 35 cycles on a Perkin Elmer Cetus DNA Thermal Cycler.

Newborn mice do not have hair. Therefore, tail snips were the source of DNA for genotyping mice younger than 14 days. DNA was extracted from tail snips using QIAamp DNA Mini Kit (catalog number 51306). The total amount of DNA in a 10- μ l PCR was 0.2 μ g.

2.3. Food for mice

Solid food pellets were purchased from Harlan Teklad, Madison, WI. Harlan Teklad LM-485 Irradiated Mouse Sterilizable Diet 7012, catalog #7912, contains 5% fat. Harlan Teklad S-2335 Irradiated Mouse Breeder Sterilizable Diet 7004, catalog #7904, contains 11% fat. A list of components of the Harlan Teklad diets can be found at <http://www.harlan.com>. Liquid food was purchased from a local grocery or drugstore, and later, 30 cases at a time (24 \times 8-oz cans per case) from Abbott Laboratories (1-800-222-6883). The liquid food is manufactured by Abbott Laboratories, Ross Products Division, Columbus, OH. Ensure Light[®], vanilla flavor, catalog # 52770; Ensure Plus[®], vanilla flavor, catalog # 50464; Ensure Fiber with FOS[®], vanilla flavor, catalog #50650.

Ensure is a complete food for a human being, containing all essential vitamins, minerals, folic acid, choline, and other essential nutrients. Ensure Plus has the highest number of calories and the highest fat content, at 360 calories and 11 g fat per 8 fl oz (236.5 ml). Ensure Fiber has 250 calories and 6 g fat per 236.5 ml; in addition, it has 4 g of fiber. Ensure Light has 200 calories and 3 g fat per 236.5 ml. The ingredients in each type of Ensure are described at <http://RPDIND01.ROSS.COM/-85256404006C18D6/>.

2.4. Containers for liquid food

Liquid food was fed to lactating dams through a glass bottle (20-ml glass scintillation vial) fitted with a one-hole rubber stopper and glass tube. The bottle was inserted into the wire cage top so that the glass tube protruded into the cage. An alternative method, that of suspending the bottle inside the cage from a bottle hanger, was unsatisfactory because many dams buried the bottle with bedding. Since nullizygotes were unable to eat solid food or lift their heads to drink from a suspended bottle, liquid food for weaned nullizygotes was placed in a small Petri dish on top of paper towels. Paper towels were used as bedding because standard bedding was kicked into the Petri dishes, soaking up the food. Paper towels were replaced daily. Food containers were washed daily.

2.5. Body temperature maintenance

One to three nullizygotes were housed in standard plastic mouse cages with a wire top. Alternatively, up to eight nullizygotes were housed in a standard hamster cage. Two plastic box tops (top of a box of 200 μ l pipette tips, 12 \times 8.3 \times 3.2 cm) were inverted and placed inside the hamster cages to provide warmth and a place to hide. A hole was cut into one side of each plastic box top to allow entry, and the boxes were lined with paper towels. Most nullizygotes were incapable of making a nest; therefore nesting material was not given to nullizygotes. Nullizygotes between the ages of 15 and 22 days required additional measures to stay warm. They were placed in cages that rested partially on an 11 \times 13 inch heating pad (purchased from Osco Drugs), providing a temperature of 42.3 °C at that end of the cage floor.

2.6. Thermometer

The axial body temperature of mice was measured with a digital thermometer, Thermalert model TH-5 and a surface Microprobe MT-D, Type T thermocouple (Physitemp Instruments Inc., Clifton, NJ). A surface probe was used because very young mice are too small to allow the use of an anal probe. AChE $-/-$ mice were handled every day for measurement of temperature and weight. A drop in temperature and body weight was an indicator of failure to thrive.

2.7. Grip strength

The device for measuring grip strength consisted of a screen mounted on a rod that could be rotated 180°. The mouse was placed on top of the screen, the screen was rotated 180°, and the time it took the mouse to fall off was measured. If the mouse could cling to the screen for 60 s or climbed to the top of the screen, it was scored as having normal grip strength.

2.8. Footprints

Feet were dipped in nontoxic paint and footprints recorded on white paper. Different colors were used for front and back feet.

2.9. Locomotor activity

A motion detector was made by the Instrument Shop at the University of Nebraska Medical Center. It consisted of a red-light-emitting diode which sent a beam of light through the cage wall, a photodiode detector on the opposite side of the cage, and a microprocessor. When the mouse passed through the beam, an event was recorded by the microprocessor. After a defined time, the total number of events was printed. The beam was set up in a sound proof, dimly lit box containing the home cage. The mouse was acclimated for 24 h before beam breaks were counted.

2.10. Neurobehavioral observations

The righting reflex was used to test motor and balance functions. Mice were placed on their backs on a piece of cardboard, giving them a rough surface for better grip. The time it took to return to an upright position was recorded. The tail pinch test was used to measure pain response. Reactivity to a light pinch with metal forceps was observed. Ability to correct orientation was measured in the geotaxis test. Mice were placed on a 45° inclined plane head down, an unnatural position for mice. The mice were observed for the ability to turn around with the head facing up the incline. Balance and hind limb strength were tested by counting the number of times each mouse reared after being placed in a novel environment, that is, displaying a bipedal posture with front feet off the ground. Pupil response was measured by shining a light into the eyes of the mice and observing constriction of the pupils. Resistance to restraint was measured as resistance to being held. Tests were from McDaniel and Moser [20].

2.10. Olfaction

The ability to smell was measured by placing 0.05 g of peanut butter in one corner of a hamster cage. A mouse was placed in the diagonal corner of the cage 46 cm away. The time it took the mouse to reach the peanut butter and actively sniff it from a distance of less than 1 cm was measured.

2.11. Blood chemistry

Whole blood was collected into serum separation tubes. Serum was analyzed for listed analytes by the Omaha Animal Medical Group, Omaha, NE.

3. Results

3.1. Husbandry

3.1.1. High fat diet for dams

Food for pups consists mainly of milk on days 1–21. Therefore, the milk was enriched by feeding dams a high fat diet. Female mice had been fed 5% fat chow for 10–12 days during the time they were housed with a male mouse. Immediately after the breeding period, female mice were fed 11% fat chow. They continued to receive 11% fat food pellets during pregnancy and while pups were nursing. The diet of lactating dams was supplemented with liquid Ensure, offered in a 20-ml bottle. This strategy, in combination with hand feeding, was successful as judged by the survival of 97% of AChE $-/-$ pups to the day of weaning ($n=100$).

3.1.2. Hand feeding and weaning

Starting on postnatal day 12 and continuing until the day of weaning, all AChE $-/-$ pups were hand fed twice a day. The pup was held by the scruff of the neck and drops of Ensure, delivered with a pipette tip, were placed into its mouth. The purpose of hand feeding with Ensure was twofold. Firstly, this diet supplement increased their chance of surviving, and secondly, they became familiar with the taste of Ensure. After weaning, their food consisted entirely of Ensure, so it was necessary to acclimate them to this food, to be sure they would eat it.

Though the normal age for weaning is postnatal day 21, the AChE $-/-$ mice were weaned earlier, on postnatal day 15. On day 15, AChE $-/-$ mice were placed into a separate cage that rested partly on a heating pad. The AChE $-/-$ mice required additional warmth because they were not able to regulate their temperature by day 15. A small plastic box (12×8.3×3.2 cm) lined with a paper towel was inverted and placed inside the cage to provide extra warmth. A second reason for weaning AChE $-/-$ mice at this early age is that they need to have food available 24 h a day. They do not get enough nutrition through nursing and can starve to death if left with the dam to day 21. It was not feasible to provide AChE $-/-$ mice with Ensure in the home cage because AChE $-/-$ mice can only eat from an open dish and the Petri dish became covered with bedding.

3.1.3. Culling

Litters were culled to 5–6 pups on postnatal day 5 by removing normal pups. The AChE $-/-$ pups were easily identified by their body tremor, which was especially noticeable when the pup was laid upside down. Culling resulted in larger body size for AChE $-/-$ pups.

3.1.4. Body temperature

By day 15, AChE $+/+$ and $+/-$ pups maintained a normal body temperature of 36.7 °C, whereas AChE $-/-$

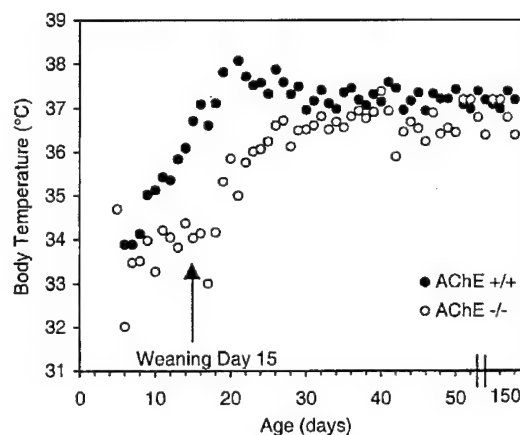


Fig. 1. Developmental delay in control of surface body temperature in AChE $-/-$ mice. Temperature of AChE $-/-$ mice (12 female+11 male) and AChE $+/+$ mice (13 female+13 male) was measured daily.

pups had an average temperature of 34 °C (Fig. 1). By day 15, the huddling time was decreased and the nesting material flattened. This caused the AChE $-/-$ mice to become hypothermic. The ability to regulate body temperature was delayed by 7 days in AChE $-/-$ mice, who reached a more normal body temperature on day 22. As shown in Fig. 1, even mature AChE $-/-$ mice had lower body temperatures than wild-type mice. The maximum surface body temperature of AChE $-/-$ mice averaged 36.5 °C, while that of AChE $+/+$ mice averaged 37.1 °C.

3.1.5. Food for AChE $-/-$ mice after weaning

Since AChE $-/-$ mice did not eat a substantial amount of solid food, liquid food was provided in the form of Ensure. There are a variety of Ensure formulations, differing in the amount of fat and calories per ml. Our initial observations had been made with Ensure Plus. To identify the Ensure that gave the highest survival rate, mice were fed three different Ensure formulations. Food consumption was measured over a period of 5 months and correlated with body weight and survival. Ensure was available to AChE $-/-$ mice 24 h a day. Fresh Ensure was provided every day in clean Petri dishes.

Fig. 2 correlates body weight with the type of Ensure in the diet. Female AChE $+/+$ mice in Fig. 2A and male AChE $+/+$ mice in Fig. 2B responded with similar gain in body weight regardless of the type of Ensure. Female wild-type mice reached a stable weight of about 27 to 32 g by day 150, while male wild-type mice reached a weight of 30–35 g. The same pattern of weight gain was observed when AChE $+/+$ mice were fed the standard 5% fat pelleted chow. Similarly, the rate of weight gain for AChE $-/-$ mice in Fig. 2C was independent of the type of Ensure. There was no difference in the rate of weight gain for male and female AChE $-/-$ mice, so the results for both genders are grouped. Adult nullizygotes are small

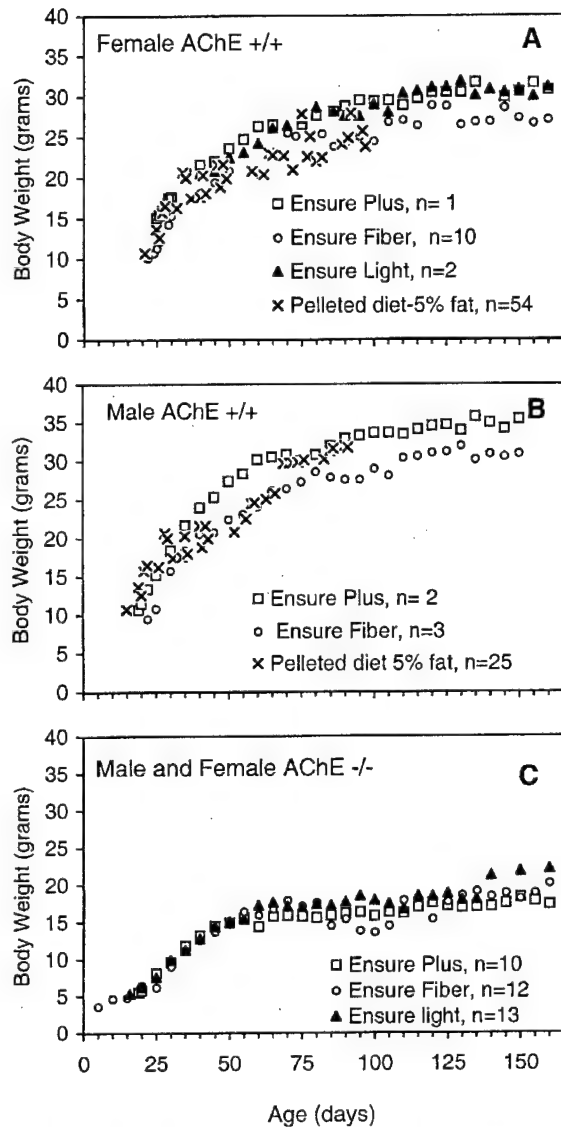


Fig. 2. Gain in body weight as a function of type of Ensure in the diet. Panel A, female AChE +/+ mice were fed Ensure Plus ($n=1$), Ensure Fiber ($n=10$), Ensure Light ($n=2$), or standard pelleted lab chow containing 5% fat ($n=54$). Panel B, male AChE +/+ mice were fed Ensure Plus ($n=2$), Ensure Fiber ($n=3$) or standard pelleted lab chow ($n=25$). Panel C, AChE -/- mice were fed Ensure Plus (4 female+6 male), Ensure Fiber (7 female+5 male), or Ensure Light (6 female+7 male).

relative to normal littermates, attaining an average body weight of about 18 g.

The rate of weight gain in AChE -/- mice was slower than in normal littermates. Fig. 3 shows that between days 6 and 14, there was either no gain in weight or there was loss of weight. This was a critical time for the AChE -/- mice. They had to be weaned to stop the weight loss and to avert death.

Survival of mice on different diets is compared in Fig. 4.

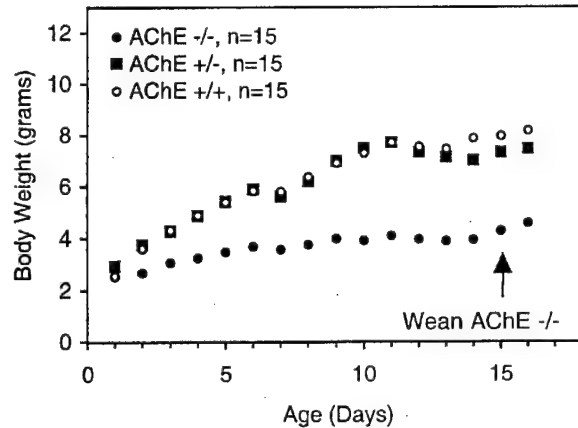


Fig. 3. AChE -/- neonates gain weight at a slower rate than wild-type and heterozygous mice. All mice were fed Ensure Fiber (6 female+9 male in each group).

All AChE +/+ mice lived longer than 250 days regardless of diet. By contrast, survival of AChE -/- mice depended on diet. The age for 50% survival of AChE -/- mice was 100 days on Ensure Fiber, 60 days on Ensure Plus, 60 days on Ensure Light, and 14 days in the absence of Ensure. Only one AChE -/- mouse from the group of 10 mice in the study has survived past 250 days, and that mouse is on Ensure Light. This mouse was euthanized at the age of 470 days. It was concluded that all three types of Ensure had similar beneficial effects, though Ensure Fiber gave a better average survival rate. Ensure Fiber had

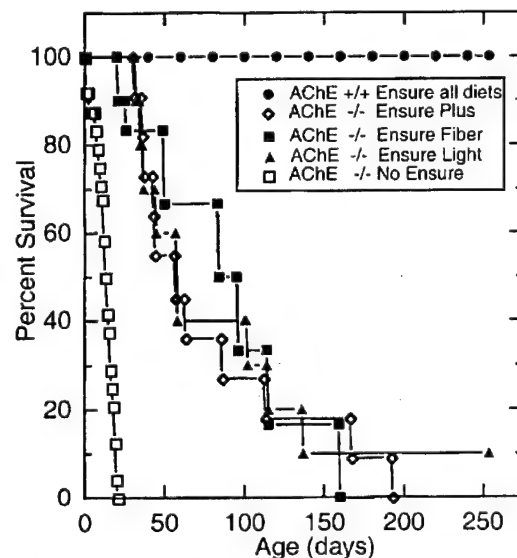


Fig. 4. Survival of AChE -/- mice depends on diet. AChE -/- mice were fed Ensure Plus (5 female+6 male), Ensure Fiber (5 female+4 male), Ensure Light (5 female+5 male), or no Ensure (11 female+13 male). All AChE +/+ mice (13 female+7 male) survived regardless of the type of Ensure they ate.

Table 1

Food consumed by wild-type (AChE +/+) and knockout (AChE -/-) mice. Calories consumed per gram of body weight per day

Age (days)	Ensure Fiber		Ensure Light		Ensure Plus	
	AChE +/+ (n=4)	AChE -/- (n=9)	AChE +/+ (n=3)	AChE -/- (n=10)	AChE +/+ (n=3)	AChE -/- (n=11)
16–40	0.86	1.01*	0.79	0.87	0.94	1.12*
41–80	0.60	0.73*	0.59	0.72*	0.60	0.74*
81–120	0.56	0.66*	0.44	0.67*	0.50	0.78*
121–160	0.53	0.70*	0.42	0.67*	0.48	0.80*

*Significantly different from AChE +/+ $P=0.02$ by single factor ANOVA.

the additional advantage of supplying fiber. Ensure Fiber was selected as the standard food for AChE -/- mice.

3.1.6. Fecal plug

AChE -/- mice between the ages of 15 and 22 days always chose the warmest spot in the cage, nesting in the area of the cage warmed by the heating pad. Mice on the heating pad often formed a fecal plug. Feces dried on the outside of the anus, blocking exodus of new feces. Mice were checked for the presence of fecal plugs daily. The fecal plug was softened with water and removed with tweezers. Voluminous soft feces flowed out after the plug was removed. Fecal plugs did not form after AChE -/- mice were removed from the heating pad.

For comparison, wild-type mice were separated from their mothers starting on postnatal day 13. Their housing was similar to that of AChE -/- mice. The food available to them was Ensure in a dish as well as solid food pellets on the cage floor. The 13–20-day-old wild-type mice also chose to nest in the area of the cage warmed by the heating pad. However, wild-type mice never developed a fecal plug.

3.1.7. Teeth

AChE -/- mice developed incisors at the same rate as their littermates. The presence of teeth rules out one possible explanation for their inability to eat solid food. They are capable of using their teeth for some gnawing, as evidenced by the shredding of paper towels. Incisors of normal mice remain worn down by chewing food pellets. Since the AChE -/- mice eat only liquid food, their front

teeth can grow excessively long and become misshapen. In some mice, the teeth had to be trimmed every day to prevent penetration into the soft tissues of both the upper and lower jaw.

3.1.8. Calories consumed per gram of body weight

Food consumption was measured daily for 5 months by weighing the amount of Ensure consumed, and correcting for evaporation. Table 1 compares calories consumed per gram of body weight per day for AChE +/+ and -/- mice on three different diets. Younger animals consumed more calories per gram of body weight than older animals. Food consumption was similar for all three types of Ensure. The important difference between AChE +/+ and -/- mice was that AChE -/- mice consumed 20–50% more calories per gram of body weight per day at all ages. For example, adult AChE -/- mice in the age group 120–160 days consumed 0.70 calories per gram of body weight per day, whereas AChE +/+ mice consumed 0.53 calories per gram of body weight per day of Ensure Fiber. The requirement for more calories suggests that AChE -/- mice have a higher metabolic rate, or that they have decreased absorption of nutrients.

3.1.9. Blood chemistry

Blood analytes were tested to determine the physiologic status of AChE -/- mice. In semi-starvation and malnutrition the levels of glucose, total protein, phosphorus, albumin, cholesterol, and potassium may be low, while blood urea nitrogen is high [12]. Table 2 shows that blood

Table 2

Analysis of serum from adult mice

Component	AChE +/+	AChE -/-
Glucose, mg/dl	165.0 (S.D. 1.7) (n=2)	164.7 (S.D. 31.2) (n=5)
Total protein, g/dl	5.4 (S.D. 0.3) (n=2)	5.5 (S.D. 0.9) (n=4)
Blood urea nitrogen, mg/dl	20.1 (S.D. 3.4) (n=2)	17.5 (S.D. 4.9) (n=4)
Phosphorus, mg/dl	10.7 (S.D. 0.1) (n=2)	9.2 (S.D. 1.4) (n=3)
Albumin, g/dl	2.42 (S.D. 0.11) (n=2)	2.57 (S.D. 0.54) (n=4)
Cholesterol, mg/dl	109.9 (n=1)	106.0 (S.D. 10.5) (n=2)
Sodium, mmol/l	155.5 (S.D. 1.63) (n=2)	139.85 (S.D. 7.14) (n=2)
Potassium, mmol/l	11.39 (S.D. 4.9) (n=2)	11.14 (S.D. 0.41) (n=2)

S.D., standard deviation.

components were similar in wild-type and AChE $-/-$ mice, thus giving no indication of malnourishment.

3.1.10. Breeding

The AChE knockout colony is maintained by breeding heterozygote males and females. We keep 50 female and 20 male AChE $+/-$ breeders. The female AChE $+/-$ breeders are 56 days to 1.5 years old, while the male breeders are 56 days to 2 years old. The average 129Sv female produces six litters in her lifetime, ranging up to eight. The litter sizes range from three to 12, and average 6.5; 15% of living newborns are AChE $-/-$. The females are bred approximately once every 2 months. This protocol yields 40–50 AChE $-/-$ mice every 2 months.

3.2. Behavior

3.2.1. Home cage behavior

Normal mice select one remote area of their cage for defecation and urination. They avoid this area. By contrast, AChE $-/-$ mice defecate and urinate in their nest. This unusual behavior suggests that higher brain function in AChE $-/-$ mice is impaired, as in dementia, or is undeveloped as in neonates.

The function of the paper towel that lines the plastic box is to absorb urine. We started lining their houses with paper towels after we noticed that AChE $-/-$ mice were shredding moist paper towels and stuffing the shreds into the top and sides of their plastic box. This activity decreased after we lined their houses.

AChE $-/-$ mice, like normal mice, are sociable. Up to eight mice in a hamster cage crowd inside one plastic box. Each hamster cage has two plastic boxes. The group of mice moves to the second box after the paper towels in the first house are soaked with urine.

3.2.2. Vocalization

About 20–25% of AChE $-/-$ mice make a bird-like chattering sound when there is a disruption in the environment, for example when the paper towels are being replaced in their cage. They do not chatter when they are nesting. Chattering begins around the time of weaning, but rarely at an earlier age. Chattering is not necessarily accompanied by signs of illness, though it is a sign of stress. Normal mice do not vocalize unless they are in distress, and then the sound they emit is a squeak. AChE $-/-$ mice squeak under exceptional circumstances, for example when they are injected with a drug. AChE $-/-$ mice make a third type of sound, a sharp chirp when they appear to suffer chronic pain.

3.2.3. Grip strength

Grip strength was measured by counting the seconds a mouse could hold on to an inverted screen before falling off. Fig. 5 shows that on postnatal day 11, all mice had poor grip strength, regardless of genotype. By day 17, the

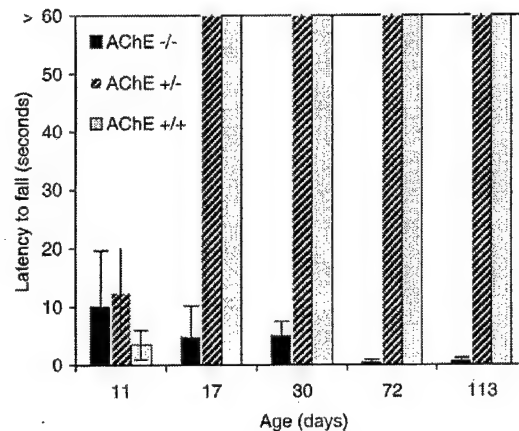


Fig. 5. Grip strength measured on an inverted screen. AChE $+/+$ (2 female+1 male), AChE $+/-$ (2 females+1 male), AChE $-/-$ (7 females+7 male) for the various age groups. Error bars show standard deviation.

AChE $+/+$ and $+/-$ mice had acquired normal grip strength. However, AChE $-/-$ mice never demonstrated improvement in their grip strength. By postnatal day 113, AChE $-/-$ mice were weaker than on day 11. These results demonstrate that the muscles required for grip are weak in AChE $-/-$ mice.

3.2.4. Gait

The abnormal gait of AChE $-/-$ mice is illustrated in Fig. 6 in the pattern of footprints. Wild-type mice leave a

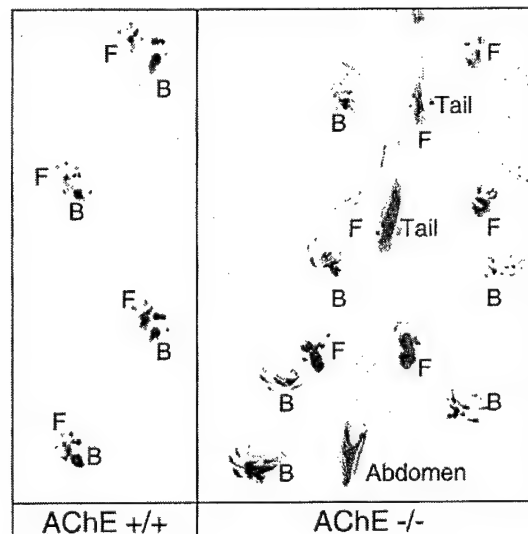


Fig. 6. Footprints. Front (F) and back (B) footprints of AChE $+/+$ mice fall close to each other in a tight pattern. By contrast, front and back footprints of AChE $-/-$ mice are far apart. The foot splay is reflected in the large horizontal distance between prints. The abdomen and tail dragged through the paint. AChE $+/+$ and AChE $-/-$ male mice of similar body weight (23 g) were selected for this experiment.

narrow trail of footprints, with the front and back prints falling nearly on top of each other. By contrast, AChE $-/-$ mice leave a wide trail of footprints, due to the splayed position of their feet. AChE $-/-$ mice drag their tail, shown in Fig. 6 as a streak of paint in the center of the pattern. Older AChE $-/-$ mice walk with their abdomen very close to the ground. They have a hump in their back, giving them a hunched posture.

3.2.5. Locomotor activity

The AChE $-/-$ mice appeared to be more sedentary than AChE $+/+$ mice. AChE $-/-$ mice slept in their plastic box during simulated daylight hours, and came out only to eat. The juvenile play activity and territorial interactions common to wild-type mice were not noticed in AChE $-/-$ mice. To quantitate these observations, locomotor activity was measured for two age groups. Fig. 7A compares locomotor activity of AChE $+/+$ and $-/-$ mice, age 23–50 days. Both genotypes showed the pattern common to nocturnal animals, that is, highest activity at night, and lowest during the day. However, the activity level was lower in the AChE $-/-$ mice for both the light and dark periods. Fig. 7B compares locomotor activity for mice, age 77–246 days. As in the younger group, mice were least active during the day light hours of 08:00 to 16:00 h and AChE $-/-$ mice were less active than AChE $+/+$ mice. Comparison of Fig. 7A and B shows that younger animals were more active than older animals, but this effect of age was more obvious in wild-type mice.

3.2.6. Development of righting reflex

AChE $-/-$ mice were slower to develop the righting reflex than their normal littermates (Fig. 8). By postnatal day 12, the littermates righted themselves within 1 s. However, AChE $-/-$ mice did not acquire this level of righting ability until day 18.

3.2.7. Sexual dysfunction

AChE $-/-$ mice are expected to be fertile because sperm have been found in the seminiferous tubule of males, and evidence of estrous has been found in females. Vaginal swabs yielded a variety of epithelial cells from cuboidal to cornified over a 4–6-day period. Normal female mice first enter estrous at 6–7 weeks of age, whereas AChE $-/-$ females have estrous at 15–16 weeks of age, 9 weeks late. In normal male mice the testes descend at 4 weeks, whereas in AChE $-/-$ males the testes descended late at 7–8 weeks. Despite these indicators of potential fertility, AChE $-/-$ mice did not become pregnant. Male and female AChE $-/-$ mice are housed together continuously during their life, but no mating behavior has been noticed. The males do not investigate female genitalia, do not mount, and do not groom females. It is possible that AChE $-/-$ mice have a defect in the production of sex hormones or have stress-related infertility [22].

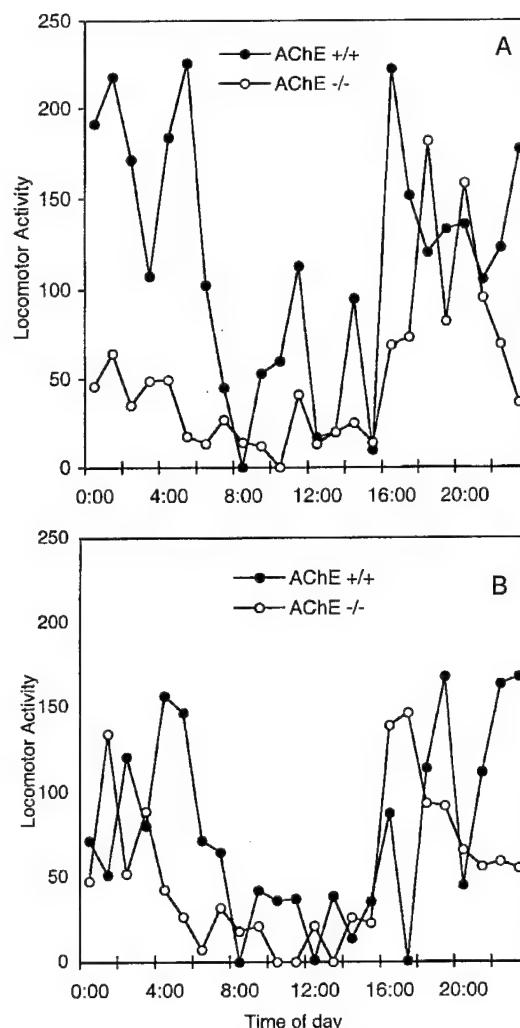


Fig. 7. Locomotor activity. Panel A, mice are 23–50 days old. Panel B, mice are 77–246 days old. $n=5$ in each group; all males. Lights are on for 12 h, from 06:00 in the morning to 18:00 h in the evening.

3.2.8. Smell

The failure of AChE $-/-$ mice to mate suggested the possibility that they might have a defect in olfactory sensation. This possibility was tested by measuring their response to a novel food substance with a strong, attractive smell, namely peanut butter. Adult mice of each genotype and sex, 10 in each group, were tested. The time it took the mice to find and sniff the peanut butter ranged from 4 s to 4 min, and averaged 1.2 ± 1.1 min for AChE $+/+$, 1.0 ± 0.8 min for AChE $+/-$, and 1.0 ± 1.0 min for AChE $-/-$ mice. It was concluded that AChE $-/-$ mice have normal olfactory sensation.

3.2.9. Stress

In response to prolonged restraint, AChE $-/-$ mice showed signs typical of cholinergic toxicity. The eyes

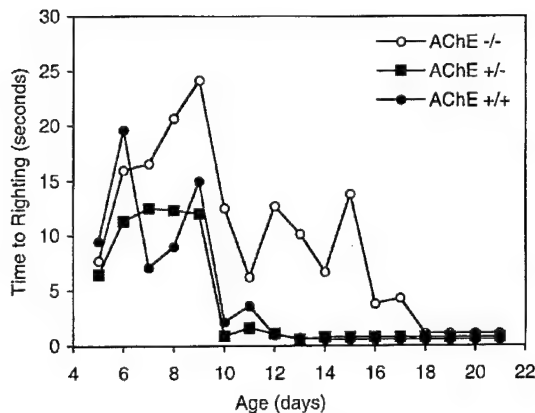


Fig. 8. Righting reflex as a function of age. The time from lying on the back to standing was measured for AChE $-/-$ (23 female+25 male), AChE $+/-$ (17 female+16 male), and AChE $+/+$ (7 female+7 male) mice. The mice had been fed Ensure Fiber.

clouded over with a thick mucus secretion, saliva wet the outside of the mouth and face, and body tremor intensified. If the mouse was not immediately released and allowed the comfort of a dark hiding place, it developed whole body seizures. AChE $-/-$ mice often recovered from seizures. Alternatively, seizures progressed to tonic convulsions where the mouse body was propelled up to 30 cm above the lab bench. In most cases tonic convulsions resulted in death.

The daily handling of the mice to measure temperature and weight did not induce seizures. Seizures have been induced in some mice by sudden exposure to light, for example when the plastic box was lifted off the nest for its daily change of paper lining. On rare occasions a mouse has had seizures after it was placed into a novel environment.

AChE $-/-$ mice were also susceptible to seizures and convulsions in their normal environment. Evidence that death had resulted from seizures and convulsions was the posture of the dead mouse: the front paws were curled under and the hind legs were extended. The stimulus that

induced the convulsions is unknown, but it is clear that AChE $-/-$ mice are sensitive to stress factors such as light, noise, and disruption of their normal environment.

3.2.10. Territorial aggressive behavior

Normal male mice housed together develop a social dominance hierarchy in which the dominant male defends the cage territory by attacking other males [5]. In these situations, dominant and submissive posturing is displayed. The AChE $-/-$ male mice are not aggressive toward other male mice and do not demonstrate posturing behavior. However, there is a social dominance in AChE $-/-$ mouse colonies, as demonstrated by barbering of whiskers, and loss of swatches of hair from the face, back and shoulders.

3.2.11. Defensive behavior

The normal instinct to bite when hurt or in distress is not seen in AChE $-/-$ mice. Although these mice have teeth, they do not bite other mice or the handler even when provoked. They display almost no resistance when held.

3.2.12. Neurobehavioral screening

The literature overwhelmingly subscribes to the idea that the acute neurotoxicity of organophosphorus pesticides and other anti-cholinesterase agents results from the inhibition of AChE catalytic activity [18,24,29,33]. We reasoned that abnormal behaviors attributed to inhibition of AChE catalytic activity in wild-type mice, could be classified as behaviors due to loss of AChE catalytic activity in AChE $-/-$ mice.

Behaviors that reflect neurotoxicity [20] were compared in adult AChE $+/+$, $+/-$, and $-/-$ mice (Table 3). Mice with zero AChE activity were clearly different on several measures. All had whole body tremor, splayed feet, hunched back, and pinpoint pupils that did not respond to light. Older AChE $-/-$ mice did not rear. Most AChE $-/-$ mice did not move in the home cage unless provoked, but remained hidden inside their plastic box. When AChE $-/-$ mice were held they did not struggle. They had little or no response when their tails were

Table 3
Neurobehavioral screening of 60–100-day-old mice of various AChE genotypes. There were 16 mice of both sexes in each genotype

Phenotype	AChE $+/+$	AChE $+/-$	AChE $-/-$
Mild whole body tremors	0/16	0/16	16/16
Hind legs splayed	0/16	0/16	16/16
Hunched back	0/16	0/16	16/16
Pupil response	16/16	16/16	0/16
Rearing (3–4 per min)	11/16	11/16	0/16
Unprovoked activity	15/16	16/16	1/16
Resistance to being restrained	16/16	15/16	2/16
Tail pinch response	15/16	15/16	2/16
Piloerection	0/16	0/16	3/16
Vocalization	0/16	0/16	4/16
Geotaxis	16/16	16/16	16/16
Righting reflex	16/16	16/16	16/16

pinched. AChE $-/-$ mice that vocalized and displayed piloerection were also noticed to have bloating in the gastrointestinal tract. All adult AChE $-/-$ mice had a normal response in the geotaxis test and all had the righting reflex. Mice with 50% of the normal AChE activity, AChE $+/-$, were indistinguishable from wild-type mice in behavioral tests. It was concluded that body tremor, pinpoint pupils, muscle weakness, and reduced pain response could be attributed to the absence of AChE catalytic activity in AChE $-/-$ mice.

4. Discussion

4.1. Starvation due to weak muscles

In this report we have solved the problem of neonatal death in the AChE $-/-$ mouse. Their average life expectancy has been extended to 100 days, from the 14 days in our first report [35]. The key to longer life was the realization that AChE $-/-$ mice were starving to death under conditions in which their littermates thrived. The explanation for why only AChE $-/-$ mice were starving is that AChE $-/-$ mice have weak muscles. Their muscles are too weak to suckle enough milk from the dam's teats. When the fat content in the dam's diet was increased, the nullizygotes consumed more calories for the same effort, allowing them to survive longer. Hand feeding, early weaning, and regulating the ambient temperature also improved their survival.

Evidence for weak muscles in the AChE $-/-$ mice includes their lack of grip strength, their abnormal posture and gait, their inability to eat solid food, inability to lift the head to drink from a suspended bottle, their low locomotor activity level, and lack of resistance to restraint. Weak muscles can be explained by malfunction of nerve impulse transmission at the neuromuscular junction, similar to that seen in endplate AChE deficient humans [10] and COLQ $-/-$ mice [8].

4.2. Are adult AChE $-/-$ mice malnourished?

On visual inspection, adult AChE $-/-$ mice appear well nourished. They have a shiny, full coat of hair, and look plump. They have abundant fat in the abdominal cavity and in subcutaneous tissue. There are no abnormalities in the levels of blood components. The blood pressure and heart rate are normal. The mouse produces abundant fecal pellets and does not have diarrhea. Thus, the adult AChE $-/-$ mouse does not have characteristics reported in semi-starvation and malnourishment [12,19].

However, the adult AChE $-/-$ mouse also exhibits traits associated with under-nutrition including low body weight, low body temperature, limited locomotor activity, no grip strength, and sexual dysfunction. Some of these

traits can be attributed directly to the absence of AChE and do not need a nutritional explanation. The absence of grip strength is due to abnormal muscle function, and the abnormal muscle function is explained by lack of AChE. The limited locomotor activity is a consequence of poor muscle function.

Other traits have no obvious connection to AChE, and may be an effect of under-nutrition. For example, the low body weight could be due to poor absorption of nutrients through the gastrointestinal tract. Nullizygotes consume more calories per gram body weight than wild-type mice, so poor feeding is not an explanation for low body weight. Hyper metabolism is another possible explanation for low body weight. If absence of AChE catalytic activity results in malabsorption of nutrients, then an explanation for how this could come about may be the following. Absence of AChE causes accumulation of excess acetylcholine. Excess acetylcholine causes a reduction in muscarinic receptors and this in turn decreases intestinal motility. The consequence of decreased intestinal motility might be malabsorption.

Another hypothetical scenario is based on the observation that AChE $-/-$ mice, unlike wild-type mice, do not eat feces. Their lack of coprophagic behavior can be attributed to their weak muscles, which makes them incapable of chewing. The possibility exists that not being coprophagic results in an absence of normal microflora, and consequently under-nutrition. If the AChE $-/-$ mice are undernourished then the degree of malnutrition is mild.

4.3. Role of AChE in development

The driving force for making the AChE knockout mouse and for prolonging its life to adulthood was the question of the nonclassical role of AChE during development [1–4,9,11,13–16,23,25,26,28,30–32]. The literature has abundant evidence that AChE has a second function, independent of its catalytic activity, and that this second, nonenzymatic role is most pronounced during development. Reviews on this topic are by Bigbee et al. [3] and Soreq and Seidman [31]. A summary of some of the evidence follows. AChE is specifically expressed in those areas of the rat thalamus and at those times when axons are projecting to the cortex. Once the nerves have grown to their destination in the cortex, AChE activity is extinguished. It has been hypothesized that AChE is a morphogen, guiding the growth of axons to those areas of the cortex involved with hearing, vision, and sensory response [25,26]. Studies in cultured neuronal cells have shown that binding of monoclonal antibody to AChE reduces neurite outgrowth [3], suggesting a morphogenic role for AChE. Inhibition of AChE activity in neuronal cultures has no effect on neurite outgrowth if the inhibitor binds at the bottom of the active site gorge, for example when the inhibitor is diisopropylfluorophosphate [3,30]. However,

an inhibitor that binds near the surface of the AChE protein, at the peripheral site, inhibits neurite outgrowth [3,15,23,28,32]. These results as well as the high sequence homology of AChE and cell adhesion proteins, have led to the hypothesis that the neuritogenic ability of AChE is mediated through a cell adhesion mechanism.

The most compelling evidence for a nonclassical function for AChE comes from studies of mutant zebrafish [2]. Behra et al. showed that AChE catalytic activity is required for neurite outgrowth in the zebrafish and that the structure of muscle fibers and of the neuromuscular junction was perturbed in zebrafish that had AChE protein but no AChE enzyme activity. Misrouting of primary motor neurons was attributed to accumulation of excess acetylcholine. Mutant zebrafish developed abnormally, had impaired motility, and died at early larval stages.

It was hoped that a mouse with no AChE protein would have obvious physical defects, for example abnormal brain structure, and would thus support the idea that AChE has a function in axon guidance during development. However, sections of brain olfactory mucosa, retina, cochlea, and striatum examined under light microscopy showed no structural abnormalities [35]. To date no axon tracing studies have been performed so it is unknown whether axon projections to the visual, auditory, and sensory cortex are normal. Another approach to this question is to test the ability of the AChE $-/-$ mouse to see, hear, and sense. Detailed studies evaluating these senses are not complete, however AChE $-/-$ mice startle from loud noise and bright light. When the prototypic neural cell adhesion molecule, N-CAM, was knocked out of the mouse, the phenotype of the knockout was mild [6]. It would not be surprising therefore, if the morphogenic function of AChE were compensated by other proteins in the mouse.

The AChE $-/-$ mouse is characterized by postnatal developmental delay. Though the mouse eventually grows to the size of an adult, it never behaves like an adult mouse. It does not learn to defecate and urinate outside the nest, and it does not become sexually mature. The phenotype of the adult AChE $-/-$ mouse provides evidence that AChE has a role in timely physical and central nervous system development. The fact that mice can live to adulthood in the complete absence of AChE enzyme and AChE protein shows that the functions of AChE are compensated. It has been speculated that the related enzyme, butyrylcholinesterase, compensates for the absence of AChE catalytic activity in nerve synapses [2,17,21].

4.4. The AChE $-/-$ mouse as a model for intoxication by anti-cholinesterases

AChE is thought to be the physiologically important target of organophosphorus pesticides, chemical nerve agents, and anti-cholinesterase pharmaceuticals

[18,24,29,33]. Acute inhibition of AChE to levels below 90% of normal leads to death. AChE knockout mice with zero AChE enzyme activity are alive, suggesting that adaptation to the absence of AChE occurred during development.

Does the phenotype of the AChE $-/-$ mouse resemble that of the wild-type mouse poisoned with anticholinesterase agent? Wild-type mice poisoned with an organophosphorus nerve agent [7] have characteristics in common with untreated AChE knockout mice. The common characteristics are loss of AChE catalytic activity, the presence of body tremor, muscle weakness, susceptibility to seizures, reduced pain response, and pinpoint pupils. When stressed, AChE $-/-$ mice salivate excessively and secrete a mucus covering on the eyes. Salivation and lacrimation are typical signs of anticholinesterase toxicity. We conclude that the AChE $-/-$ mouse has many of the characteristics of the anticholinesterase intoxicated mouse, and will be useful as a model for gene and protein therapy studies aimed at treating toxicity.

The heterozygote AChE $+/-$ mouse has 50% of the normal AChE activity [17]. Despite this deficiency, the mouse appears to be normal. One characteristic that distinguishes it from wild-type mice is a greater sensitivity to the toxic effects of organophosphorus poisons [7,35]. This feature is the basis for our prediction that humans partially deficient in AChE will be identified in the future, and that their health may be compromised by low doses of organophosphorus pesticides that have no ill effects on the general population.

Acknowledgements

We thank Virginia C. Moser at the Environmental Protection Agency, Research Triangle Park, North Carolina for suggesting we feed our mice Ensure; Christopher J. Gordon at the Environmental Protection Agency for suggesting measuring body temperature; Ramona M. Rodriguez and William C. Wetsel at Duke University for demonstrating measurement of righting reflex and footprints; Clarence A. Broomfield at the US Army Institute of Chemical Defense, Aberdeen, MD for the design of the inverted screen; Lawrence M. Schopfer at UNMC for designing the single beam locomotor activity instrument; Andreea Ticu Boeck at UNMC for genotyping the mice; and Rachael Ferber at UNMC for testing righting reflex. This work was supported by US Army Medical Research and Material Command Grants DAMD17-01-1-0776 and DAMD17-01-2-0036 (to O.L.) and by a Center Grant to UNMC from the National Cancer Institute, Grant CA36727. The opinions or assertions contained herein belong to the authors and should not be construed as the official views of the US Army or the Department of Defense.

References

- [1] S. Bataille, P. Portalier, P. Coulon, J.P. Ternaux, Influence of acetylcholinesterase on embryonic spinal rat motoneurons growth in culture: a quantitative morphometric study, *Eur. J. Neurosci.* 10 (1998) 560–572.
- [2] M. Behra, X. Cousin, C. Bertrand, J.L. Vonesch, D. Biellmann, A. Chatonnet, U. Strähle, Acetylcholinesterase is required for neuronal and muscular development in the zebrafish embryo, *Nat. Neurosci.* 5 (2002) 111–118.
- [3] J.W. Bigbee, K.V. Sharma, J.J. Gupta, J.L. Dupree, Morphogenic role for acetylcholinesterase in axonal outgrowth during neural development, *Environ. Health Perspect.* 107 (Suppl. 1) (1999) 81–87.
- [4] M.F. Blasina, A.C. Faria, P.F. Gardino, J.N. Hokoc, O.M. Almeida, F.G. de Mello, C. Arruti, F. Dajas, Evidence for a noncholinergic function of acetylcholinesterase during development of chicken retina as shown by fasciculin, *Cell Tissue Res.* 299 (2000) 173–184.
- [5] J.N. Crawley, in: *What's Wrong With My Mouse? Behavioral Phenotyping of Transgenic and Knockout Mice*, Wiley-Liss, New York, 2000, pp. 167–171.
- [6] H. Cremer, R. Lange, A. Christoph, M. Plomann, G. Vopper, J. Roes, R. Brown, S. Baldwin, P. Kraemer, S. Scheff, D. Barthels, K. Rajewsky, W. Wille, Inactivation of the N-CAM gene in mice results in size reduction of the olfactory bulb and deficits in spatial learning, *Nature* 367 (1994) 455–459.
- [7] E.G. Duysen, B. Li, W. Xie, L.M. Schopfer, R.S. Anderson, C.A. Broomfield, O. Lockridge, Evidence for non-acetylcholinesterase targets of organophosphorus nerve agent; supersensitivity of the acetylcholinesterase knockout mouse to VX lethality, *J. Pharmacol. Exp. Ther.* 299 (2001) 542–550.
- [8] G. Feng, E. Krejci, J. Molgo, J.M. Cunningham, J. Massoulié, J.R. Sanes, Genetic analysis of collagen Q: roles in acetylcholinesterase and butyrylcholinesterase assembly and in synaptic structure and function, *J. Cell Biol.* 144 (1999) 1349–1360.
- [9] C. Holmes, S.A. Jones, T.C. Budd, S.A. Greenfield, Non-cholinergic, trophic action of recombinant acetylcholinesterase on mid-brain dopaminergic neurons, *J. Neurosci. Res.* 49 (1997) 207–218.
- [10] D.O. Hutchinson, T.J. Walls, S. Nakano, S. Camp, P. Taylor, C.M. Harper, R.V. Groover, H.A. Peterson, D.G. Jamieson, A.G. Engel, Congenital endplate acetylcholinesterase deficiency, *Brain* 116 (1993) 633–653.
- [11] G. Johnson, S.W. Moore, The adhesion function on acetylcholinesterase is located at the peripheral anionic site, *Biochem. Biophys. Res. Commun.* 258 (1999) 758–762.
- [12] A. Keys, J. Brozek, A. Henschel, O. Mickelsen, H.L. Taylor, in: *The Biology of Human Starvation*, Vol. 1, The University of Minnesota Press, Minneapolis, 1950, pp. 1–763.
- [13] C. Koenigsberger, S. Chiappa, S. Brimijoin, Neurite differentiation is modulated in neuroblastoma cells engineered for altered acetylcholinesterase expression, *J. Neurochem.* 69 (1997) 1389–1397.
- [14] P.G. Layer, Cholinesterases preceding major tracts in vertebrate neurogenesis, *BioEssays* 12 (1990) 415–420.
- [15] P.G. Layer, T. Weikert, R. Alber, Cholinesterases regulate neurite growth of chick nerve cells in vitro by means of a nonenzymatic mechanism, *Cell Tissue Res.* 273 (1993) 219–226.
- [16] P.G. Layer, E. Willbold, Novel functions of cholinesterases in development, physiology and disease, *Prog. Histochem. Cytochem.* 29 (1995) 1–94.
- [17] B. Li, J.A. Stribley, A. Ticu, W. Xie, L.M. Schopfer, P. Hammond, S. Brimijoin, S.H. Hinrichs, O. Lockridge, Abundant tissue butyrylcholinesterase and its possible function in the acetylcholinesterase knockout mouse, *J. Neurochem.* 75 (2000) 1320–1331.
- [18] O. Lockridge, P. Masson, Pesticides and susceptible populations: people with butyrylcholinesterase genetic variants may be at risk, *Neurotoxicology* 21 (2000) 113–126, Review.
- [19] S.L. Manocha, in: *Malnutrition and Retarded Human Development*, Charles C. Thomas, Springfield, IL, 1972, pp. 21–88.
- [20] K.L. McDaniel, V.C. Moser, Utility of a neurobehavioral screening battery for differentiating the effects of two pyrethroids, permethrin and cypermethrin, *Neurotoxicol. Teratol.* 15 (1993) 71–83.
- [21] M.M. Mesulam, A. Guillozet, P. Shaw, A. Levey, E.G. Duysen, O. Lockridge, Acetylcholinesterase knockouts establish central cholinergic pathways and can use butyrylcholinesterase to hydrolyze acetylcholine, *Neuroscience* (2002) in press.
- [22] I. Mor, D. Grisaru, L. Titelbaum, T. Evron, C. Richler, J. Wahrman, M. Sternfeld, L. Yogeve, N. Meiri, S. Seidman, H. Soreq, Modified testicular expression of stress-associated 'readthrough' acetylcholinesterase predicts male infertility, *FASEB J.* 15 (2001) 2039–2041.
- [23] F.J. Munoz, R. Aldunate, N.C. Inestrosa, Peripheral binding site is involved in the neurotrophic activity of acetylcholinesterase, *NeuroReport* 10 (1999) 3621–3625.
- [24] C.N. Pope, Organophosphorus pesticides: do they all have the same mechanism of toxicity?, *J. Toxicol. Environ. Health B Crit. Rev.* 2 (1999) 161–181.
- [25] R.T. Robertson, A morphogenic role for transiently expressed acetylcholinesterase in developing thalamocortical systems?, *Neurosci. Lett.* 75 (1987) 259–264.
- [26] R.T. Robertson, J. Yu, Acetylcholinesterase and neural development: new tricks for an old dog?, *News Physiol. Sci.* 8 (1993) 266–272.
- [27] E.M. Schmitteckert, C.M. Prokop, H.J. Hedrich, DNA detection in hair of transgenic mice—a simple technique minimizing the distress on the animals, *Lab. Anim.* 33 (1999) 385–389.
- [28] K.V. Sharma, C. Koenigsberger, S. Brimijoin, J.W. Bigbee, Direct evidence for an adhesive function in the noncholinergic role of acetylcholinesterase in neurite outgrowth, *J. Neurosci. Res.* 63 (2001) 165–175.
- [29] F.R. Sidell, Clinical effects of organophosphorus cholinesterase inhibitors, *J. Appl. Toxicol.* 14 (1994) 111–113.
- [30] D.H. Small, G. Reed, B. Whitefield, V. Nurcombe, Cholinergic regulation of neurite outgrowth from isolated chick sympathetic neurons in culture, *J. Neurosci.* 15 (1995) 144–151.
- [31] H. Soreq, S. Seidman, Acetylcholinesterase—new roles for an old actor, *Nat. Rev. Neurosci.* 2 (2001) 294–302.
- [32] M. Srivatsan, B. Peretz, Acetylcholinesterase promotes regeneration of neurites in cultured adult neurons of *Aplysia*, *Neuroscience* 77 (1997) 921–931.
- [33] P. Taylor, Anticholinesterase agents, in: J.G. Hardman, L.E. Limbird (Eds.), 10th Edition, Goodman & Gilman's *The Pharmacological Basis Of Therapeutics*, McGraw Hill, New York, 2001, pp. 175–191.
- [34] W. Xie, P.J. Wilder, J. Stribley, A. Chatonnet, A. Rizzino, P. Taylor, S.H. Hinrichs, O. Lockridge, Knockout of one acetylcholinesterase allele in the mouse, *Chem. Biol. Interact.* 119–120 (1999) 289–299.
- [35] W. Xie, J.A. Stribley, A. Chatonnet, P.J. Wilder, A. Rizzino, R.D. McComb, P. Taylor, S.H. Hinrichs, O. Lockridge, Postnatal developmental delay and supersensitivity to organophosphate in gene-targeted mice lacking acetylcholinesterase, *J. Pharmacol. Exp. Ther.* 293 (2000) 896–902.

Rescue of the Acetylcholinesterase Knockout Mouse by Feeding a Liquid Diet; Phenotype of the Adult Acetylcholinesterase Deficient Mouse

E.G. Duysen¹, J.A. Stribley², D. Fry¹, S. Hinrichs², O. Lockridge¹

¹ University of Nebraska Medical Center, Eppley Institute,

²University of Nebraska Medical Center, Department of Pathology and Microbiology,
Omaha, NE, USA

XI International Symposium on Cholinergic Mechanisms-Function and Dysfunction and
2nd Misrahi Symposium on Neurobiology, St. Moritz, Switzerland, May 5-9, 2002.

Acetylcholinesterase (AChE, EC3.1.1.7) functions in nerve impulse transmission, and possibly as a cell adhesion factor during neurite outgrowth. These functions predicted that mice with zero AChE activity would be unable to live. It was a surprise to find that AChE^{-/-} mice were born alive and survived an average of 14 days. The emaciated appearance of AChE^{-/-} mice suggested an inability to obtain sufficient nutrition and experiments were undertaken to increase caloric intake. Pregnant and lactating dams were fed 11% high fat chow supplemented with liquid Ensure®. AChE^{-/-} pups were weaned early, on day 15, and fed liquid Ensure. Nullizygous animals showed slow but steady weight gain with survival over 1 year, but remained smaller than their littermates. They demonstrated delays in temperature regulation (day 22 vs 15), eye opening (day 13 vs 12), righting reflex (day 18 vs 12), descent of testes (week 7-8 vs 4), and estrous (week 9 vs 6-7). Physical findings in adult AChE^{-/-} mice included body tremors, abnormal gait and posture, absent grip strength, inability to eat solid food, pinpoint pupils, decreased pain response, vocalization, and early death caused by seizures or gastrointestinal tract ileus. Behavioral deficits included urination and defecation in the nest, lack of aggression, reduced pain perception, and sexual dysfunction. These findings support the classical role for AChE in nerve impulse conduction and further suggest that AChE is essential for timely physical development and higher brain function. This work was supported by U.S. Army Medical Research and Materiel Command Grants DAMD17-01-1-0776 and DAMD17-01-02-0036.